UNIVERSIDADE DO ALGARVE

UNIVERSITY OF ALGARVE

FACULDADE DE CIÊNCIAS E TECNOLOGIA

FACULTY OF SCIENCES AND TECHNOLOGY

"Assessment of Sea Surface Temperatures (SST) and Seasonal upwelling in SW Portugal"

MESTRADO EM GESTÃO DA ÁGUA E DA COSTA (CURSO EUROPEU)

ERASMUS MUNDUS EUROPEAN JOINT MASTER

IN WATER AND COASTAL MANAGEMENT

(BY: NDUI AIKAYO)

FARO 2010

NOME / NAME: Aikayo, Ndui

DEPARTAMENTO / DEPARTMENT: Química, Bioquímica e Farmácia – Faculdade de Ciências e Tecnologia da Universidade do Algarve

ORIENTADOR /SUPERVISOR: **Professor Alice Newton**

Co Supervisor: **Dr. John Icely**

University of Algarve Faculty of Science and Technology (FCT)

DATA / DATE: 15-03-10

TÍTULO DA TESE / TITLE OF THESIS:

Assessment of Sea Surface Temperatures (SST) and Seasonal upwelling in SW Portugal.

JURI:

Prof. Tomasz Boski
Dr. John David Icely
Dr. Flávio Augusto Bastos da Cruz Martins
Prof. Alice Newton
Dr. Emilie Brévière

ACKNOWLEDGEMENTS

I express my acknowledgements to the Erasmus Mundus External window cooperation - Lot 10 Programme awarded by European Commission for funding the European Joint Master in Water and Coastal Management and this research.

I would like to thank my supervisors, Professor Alice Newton and Dr.John Icely (University of Algarve, Portugal) for their continuous assistance, comments, suggestions and guidance's throughout my study.

My Special thanks to the Government of the Republic of Zambia (GRZ) through the Ministry of Communications and Transport (MCT) at the Zambian Meteorological Department (ZMD), for granting me study leady to come and study this very important Master.

I extend my sincere thanks to Dr. Simon Mason of International Research Institute (IRI), for his technical assistance on the CPT software, Damian Icely on the Ferret software, MR. Faqih Akhmad of Center for Climate Risk and Opportunity Management in Southeast Asia and Pacific (CCROM-SEAP),and Department of Geophysics and Meteorology, Bogor Agriculture University ,Indonesia for installing a Microsoft version of Ferret on my Laptop, Bruno Fragoso and Sonia Cristina for their assistance on Data analysis, and sites.

I would like to thank all my friends for their love and help during my study and project work in Europe. Finally I would like to thank my parents, family and all those who have extended their help to me.

Resumo

Informação meteorológica como a Temperatura de Superfície do Mar (SST), a Direcção e Velocidade do vento, são parâmetros importantes para determinar a ocorrência de afloramento costeiro. Neste estudo são apresentadas técnicas, que podem ser usadas para determinar dados meteorológicos em falta nas bases de dados, nomeadamente das autoridades meteorológicas nacionais. O programa Climate Predictability Tool (CPT) foi usado para determinar os valores em falta nas séries de dados através da Regressão de Componentes Principais (PCR). Para calcular as relações entre as séries de dados foi usado o SYSTAT e os gráficos derivados do FERRET gerados a partir das imagens de satélite. Os resultados indicam que os valores do arquivo do www.windguru.cz para Sagres (SW Portugal), são mais adequados para substituir valores em falta de temperatura, mostrando uma relação na ordem do 88% relativamente aos dados *in situ*. Por outro lado, os gráficos gerados pelo FERRET indicam que podem ser alternativa para gerar os dados de direcção e velocidade do vento.

Em geral, o afloramento costeiro envolve processos físicos, químicos e biológicos. Em relação aos processos físicos, a água fria oriunda do fundo determina a temperatura da superfície do mar. O vento representa um papel importante na regulação da temperatura da superfície do mar e transporte do calor do oceano. A nível químico, o transporte de águas ricas em nutrientes do fundo até á superfície, promove os processos biológicos, como a ocorrência de florescências de fitoplâncton resultando num aumento de clorofila causando a alteração da côr da água, que pode ser detectada através de imagens de satélite.

Informação disponível no sítio de internet do Windguru e os gráficos do FERRET podem ser adequados para completar dados em falta das bases de dados.

Informação adicional, sobre condições meteorológicas e oceanográficas que são responsáveis pela ocorrência do afloramento costeiro, estão disponíveis neste trabalho.

Palavras-chave:

Afloramento costeiro, Temperatura das Superfície do Mar (SST), Vento, FERRET, SYSTAT, Windguru

ABSTRACT

Meteorological data such as Sea Surface Temperature (SST), Wind direction and Wind speed are important parameters to determine the occurrence of upwelling. This study demonstrates some useful techniques that can be used to provide useful meteorological data, where these may be missing from conventional data sets that are provided by, for example, national meteorological authorities. The techniques used include: Plotting the daily temperature datasets in Lines on 2Axes using EXCEL,the nearest neighbour station using Principal Component Regression in Climate Predictability Tool (CPT), calculating the skills by comparing the two datasets using SYSTAT and using FERRET satellite derived data plots to determine the missing data for a particular time. Results showed that the www.windguru.cz dataset for Sagres (SW Portugal) proved to be more suitable for replacing the missing data of temperature on the Meteorological datasets because the skills were as high as 88%, comparing with *in situ* data. FERRET plots also indicated suitable substitutes for non availability of the Meteorological data such as wind direction and speed.

In global scenario, upwelling involves the Physical, Chemical and Biological process. Physically-like cold water on the surface because of upwelling and this affects Sea surface temperature. Wind plays an important role in regulating the Sea Surface Temperature (SST) transporting heat through the surface water. Chemically - nutrients rich water brought to the surface and Biologically-production of phytoplankton bloom that results into chlorophyll increase and this gives the resulting color change in ocean color which can be detected by satellite images.

Data from the Windguru website archive and the Ferret derived plots are suitable for replacing where they are missing data on the Meteorological datasets.

Details and a short review of the oceanographic and meteorological conditions that are responsible for upwelling are presented in the text.

Keywords:

Upwelling, Sea Surface Temperatures (SST), Wind, FERRET, SYSTAT, Windguru

LIST OF ABBREVATIONS

AIRT	Air temperature
AOU	Apparent Oxygen Utilization
AVHRR	Very high resolution radiometer
AWS	Automatic weather station
CAS	Central American Seaway
CPT	Climate Predictability Tool
CZCS	Coastal Zone Color Scanner
DLESE	Digital Library for Earth System Education
ENSO	El Niño Southern Oscillation
GUI	Graphical user interface
HAB	Harmful Algal Bloom
ITCZ	Inter Tropical Convergence Zone
IRI	International Research institute for Climate and Society.
MGSVA	Mariano Global Surface Velocity Analysis
NOAA	National Oceanic and Atmospheric Administration
NAO	North Atlantic Oscillation
NAOI	Northern Atlantic Oscillation Index
NASA	National Aeronautics and Space Administration

NCOF	National Center for Oceanic Forecasting
PC	The Portugal Current
PC	Peruvian Current
PCC	The Portugal Coastal Current
PCCC	The Portugal Coastal Countercurrent
PCR	Principal Components Regression
PMEL	Precision Measurement Equipment Laboratory
SAA	South Atlantic Anticyclone
SLP	Sea Level Pressure
SPEH	Specific humidity
SOI	Southern Oscillation (ENSO) Index
SSH	Sea Surface Height
SST	The Sea Surface Temperature
STN	Station
THC	Thermohaline circulation
TMAP	Thermal Modeling and Analysis Project
UWND	Zonal wind
VWND	Meridional wind
WHWP	Western Hemisphere Warm Pool
WSPD	Wind speed
WX	Weather

TABLE OF CONTENTS

LIST OF FIGURES IN THE STUDY

LIST OF FIGURES FOR REVIEW

LIST OF TABLES –Appendix C.

1. INTRODUCTION

Coastal upwelling is a phenomenon, with dramatic effects on physical, chemical and biological processes (Sousa and Bricaud, 1992; Conway, 1997; Wollast, 1998; Harimoto *et al.*, 1999; Brogueira *et al.*, 2004; Loureiro *et al.*, 2005; Relvas *et al.*, 2007; Loureiro *et al.*, 2008). A short review of the oceanographic and meteorological conditions that are responsible for upwelling events is provided in Appendix A. Considering the profound influence of upwelling events on biological processes in the locations where they occur, it is important to have good information about meteorological and oceanographic conditions in order to understand the chemical and biological processes that occur before, during and after upwelling events. Many scientists working on these processes depend on other authorities to provide them with background information on meteorological and even oceanographic conditions. However, there are many situations where this data is incomplete. The objective of this study is to demonstrate some techniques that can be used to provide useful meteorological data, where these may be missing from conventional data sets that are provided by, for example, national meteorological authorities. This study will be based on actual data sets collected historically and recently from Sagres in an upwelling area on the SW coast of the Iberian peninsular.

2. Study Area

Sagres is on the south west coast of Portugal, located at 37°N and 8.95°W, it is located at the extreme south-west of Algarve. (Fig.1.below). Climate of the area can be divided into two; the southern Sagres has Mediterranean type which is warmer and the western part which is colder, stormy and is exposed to waves.

The coastal area is classified as a mesotidal moderately exposed coastal water of the Atlantic type (Bettencourt *et al.*, 2004). The Sagres area, off the south west coast of the

Iberian Peninsula (Fig. 1) is affected by seasonal upwelling induced by northerly winds from May to September (Wooster *et al*., 1976; Fiúza, 1983; Sousa and Bricaud, 1992).

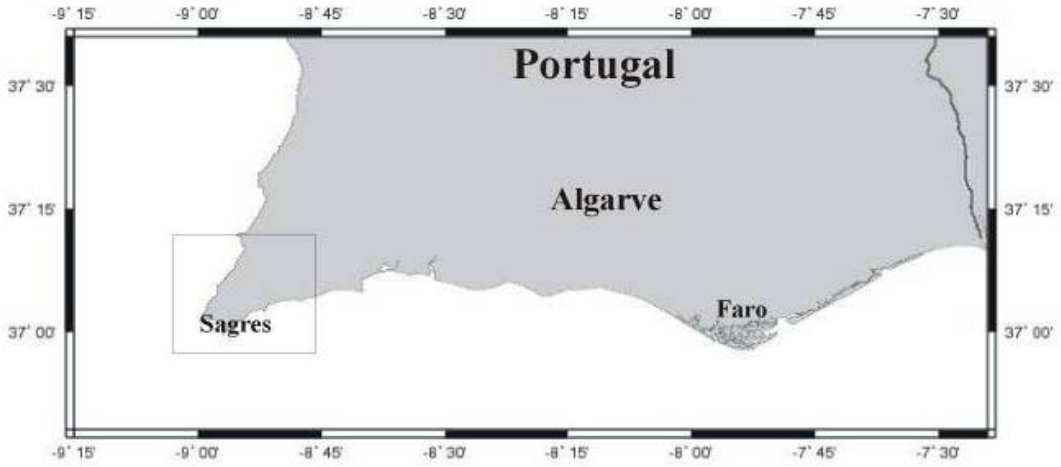

Fig.1. Maps showing the general and specific location of Sagres (Adapted from: Fragoso and Icely, 2009).

2.1. Coast of SW Portugal (Sagres)

The Portugal Current (PC) system, defines the classic strictly southerly flow regime as typically depicted in marine atlases and pilot charts, when observed at yearly time scales. The entire system extends from about 36°N to about 46°N and from the Iberian shores to about 24°W (Perez *et al.*, 2001; Martins *et al.*, 2002). The Portugal Current itself is poorly defined spatially because of the intricate interactions between coastal and offshore currents, bottom topography, and water masses. The system is comprised of the following main currents: 1) The Portugal Current, which is a broad, slow, generally southward-flowing current that extends from about 10°W to about 24°W longitude; 2) The Portugal Coastal Countercurrent (PCCC), a southward flowing surface current along the coast during downwelling season, mainly over the narrow continental shelf to about 10-11°W longitude and flow from about 41-44°N; and 3) the Portugal Coastal Current (PCC), a generally poleward current that dominates over the PCCC during times of upwelling and like the PCCC, extends to about 10-11°W from

shore, also present mainly from 41-44°N, where flow is 13.5 ± 5.7 cm s^{-1} (Perez *et al.*, 2001; Martins *et al.,* 2002). Fig. 2 shows the Portugal current system in three monthly seasonal averages. The Portugal current as represented by the Mariano Global Surface Velocity Analysis (MGSVA). The average flow is towards the south and feeds the Canary Current. Highlighted in red in the figures is the area where the coastal current can flow northward, depending on the winds The Portugal currents, has the mean pattern as well as seasonal variation and are well established despite relatively few systematic observations. The Portugal and Canary Currents form the eastern limb of the North Atlantic Subtropical Gyre (Barton, 2001).

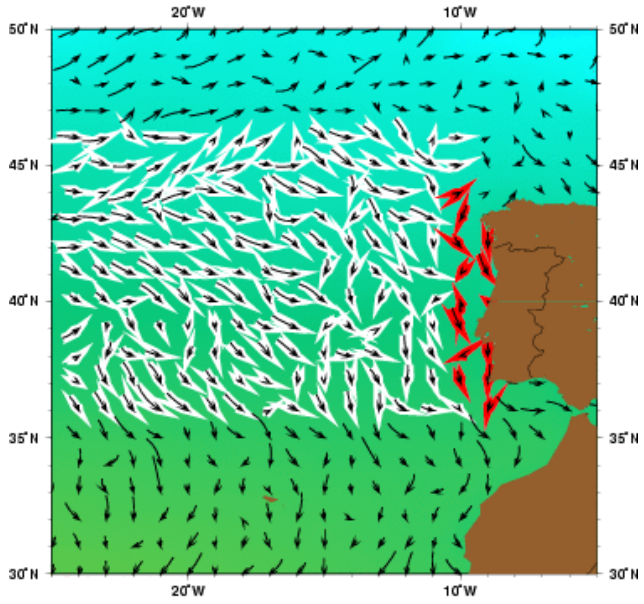

(A) Jan-Feb-Mar

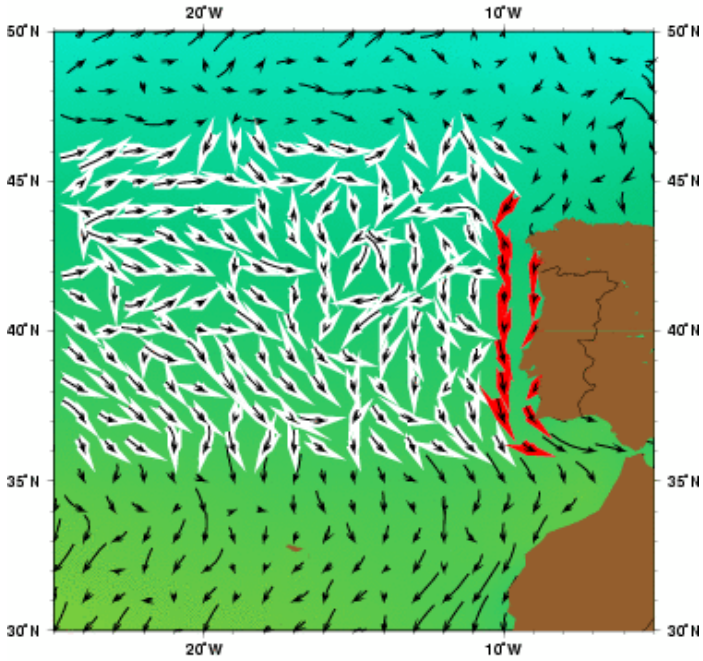

(B) Apr-May-Jun

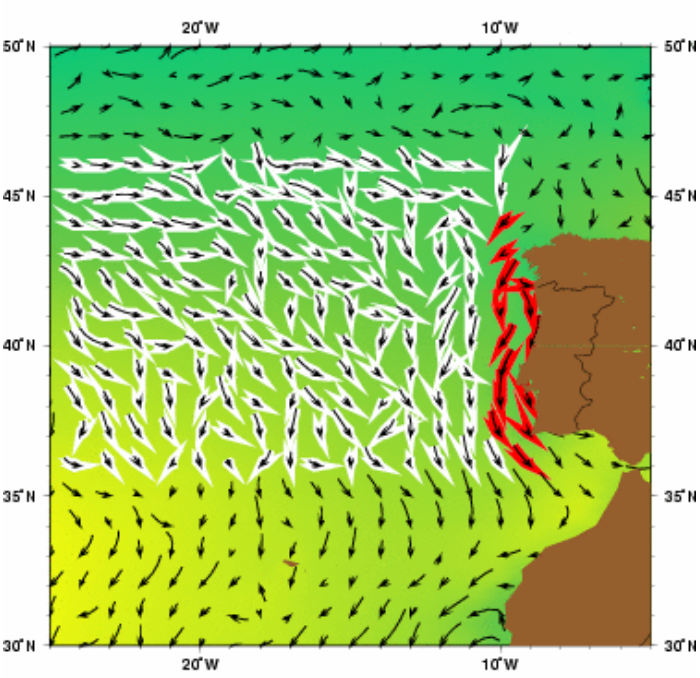

(C) Jul-Aug-Sep

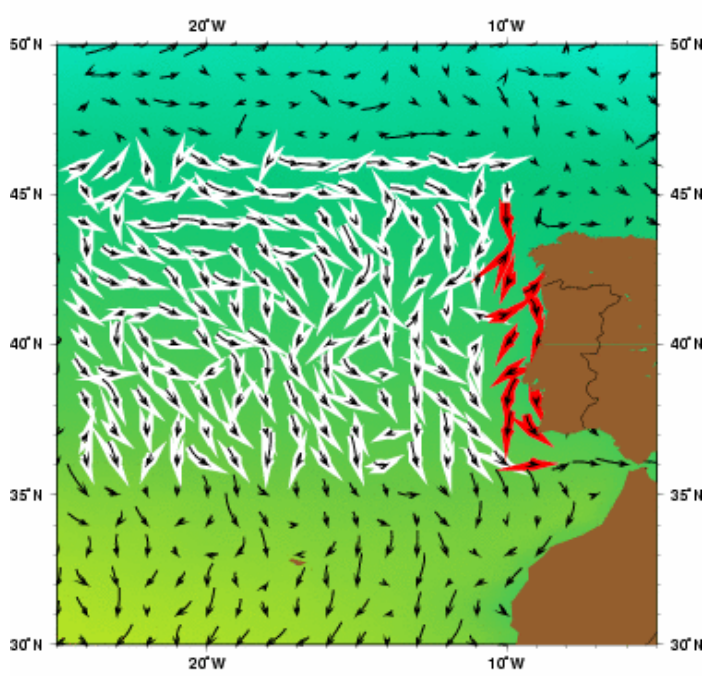

(D) Oct-Nov-Dec

Fig.2. The Portugal Current System from January to December, From: Bischof *et al.,* 2003) http://oceancurrents.rsmas.miami.edu/atlantic/portugal.html.

2.2. Upwelling along Sagres coast (SW Portugal

Upwelling takes place along the Sagres coast of Portugal during the summer under the fairly strong and steady northerly winds. Studies of Upwelling in the Portuguese coastline have been done and papers have been published on the same topic by authors such as (Santos *et al.,* 2001; Relvas and Barton, 2002; Loureiro *et al.*, 2008; Fragoso and Icely, 2009). Others are (Villa *et al.*, 1997; Peliz *et al.*, 2001; Loureiro *et al.*, 2005). Upwelling responds quickly to northerly winds, particularly south of capes, appearing first along the coastline and then spreading offshore as the event progresses (Fiúza *et al.*, 1982).The Portugal Coastal Current (PCC), extends from about 10°W to about 24°W longitude; is generally a poleward current that dominates over the Portugal Coastal Countercurrent (PCCC) during times of upwelling and like the PCCC, extends to about 10-11°W from shore, also present mainly from 41-44°N, where flow is 13.5 ±

5.7 cm s^{-1} (Perez *et al.*, 2001; Solignac *et al.*,2008). The Portugal Current system is supplied mainly by the intergyre zone in the Atlantic, a region of weak circulation bounded to the north by the North Atlantic Current and to the south by the Azores Current (Perez *et al.*, 2001).For some part of the year the north-east Trade Winds blow along every part of the subtropical Eastern boundary with a strong alongshore component that produces offshore Ekman transport in the surface layers and therefore upwelling at the coast. The strength of upwelling is conventionally expressed in terms of the upwelling (or Bakun) index, which is simply the Ekman transport $\boldsymbol{TE = (q/o f)}$ where **q** is the component of wind stress parallel to shore, **o** is the density of sea water, and $\boldsymbol{f}$ **i**s the Coriolis parameter (Barton, 2001), see Fig. 3 below.

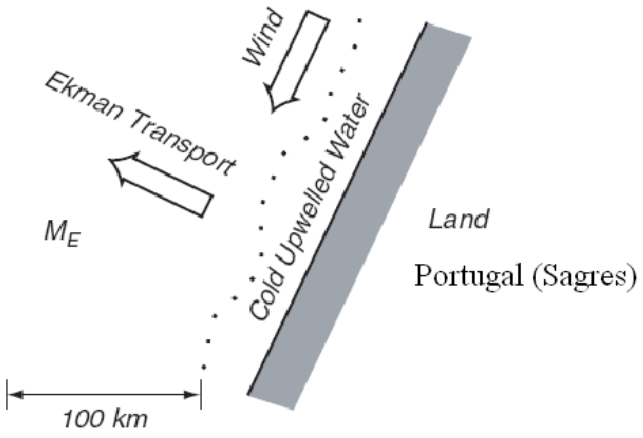

Fig.3. Showing coastal upwelling along the Sagres coastline SW-Portugal (Source Adapted from Microbiology procedure (http://www.microbiologyprocedure.com/microbial-ecology-of-different-ecosystems/marine-ecosystem-upwelling.html))

Earlier investigations on the influence of the atmospheric circulation on upwelling off Northwest Africa are expanded up to the coast off Portugal. In this area, upwelling can be found south of 40º N during summer and autumn; between 40ºN and 43ºN the upwelling period decreases with increasing latitude. The yearly amplitude of differences of sea level pressure normal to the coast which represents the synoptic scale coast

parallel wind component and offshore surface temperatures is largest in 38ºN, decreasing to the north. From empirical orthogonal functions it is suggested that off Portugal local winds induce a more intense upwelling than the winds off Northwest Africa (Detlefsen and Speth, 1980). Local winds, the continental-shelf/upper-slope bathymetry and the coastal morphology largely determines the upwelling patterns off Portugal (Fiúza, 1983). The evolution of the upwelling regime off west Portugal between 1941 and 2000 was investigated. Monthly averages of the longshore (meridional) wind component at four coastal stations of the Institute for Meteorology were computed and subject to linear regression analysis. Several comparisons were made among stations until a final regression model was reached. The resulting residuals were checked for the presence of red noise, and pairwise correlation coefficients were estimated for residuals of different stations. To complement this study, monthly sea-surface temperature averages were computed for six regions off west Portugal and subject to a similar procedure. In both analyses, it was concluded that the Portuguese upwelling regime has weakened since the 1940s. The waning of the northerly, upwelling favourable winds was significant throughout the traditional upwelling season (April-September). Sea-surface temperature showed a steady year-round increase from 1941 onwards, in both offshore (+0.002°C/year) and coastal (+0.010°C/year) regions (Lemos and Pires, 2004).

Conclusions had been made that upwelling took place seasonally along the west coast of Portugal, reaching maximum in July, August and September, under fairly steady northerly winds, and that its intensity presented a strong correlation with the north-south wind stress, with lag of a month relative to the most favorable north winds which occurred from June to August; during winter a general situation of convergence

prevailed, in apparent relation with the then predominant southerly winds (Sousa and Bricaud, 1992).

The analysis of 25 Coastal Zone Color Scanner (CZCS), derived phytoplankton pigment concentrations in Portuguese coastal waters revealed the occurrence of pigment-rich mesoscale structures which were strongly associated with the dynamics of coastal upwelling induced by favorable wind regimes along the west and the south coasts of Portugal during the summer (Sousa and Bricaud,1992).

Present studies have shown a clear pronounced nutrient dilution and contrasting Apparent Oxygen Utilization (AOU) values associated with the presence of a meddy structure in the eastern flank of Portimão Canyon off Southern Portugal. The chemical properties depict the meddy vertical extension further down the thermohaline properties, emphasizing the meddy impact on the biogeochemistry of the surrounding water masses (Brogueira *et al.*, 2004).

3. Objective of the study

The objective of this study is to demonstrate some techniques that can be used to provide useful meteorological data, where these may be missing from conventional data sets that are provided by, for example, national meteorological authorities.

This is mainly achieved by comparison of Windguru *(*www.windguru.cz) data from Sagres (SW Portugal), temperature logger and wind data with the weather station data (Dr.Icely WX.stn.) at Sagres, so as to indentify upwelling events at the coastline. FERRET software is also employed to assist in substitution of the missing data. This meteorological data is related as well as assist in interpreting the biological, chemical and physical activities that occur in the coastal upwelling. The main problem is the missing data particularly in the upwelling month of August. The aim is to test the possibility of substituting windguru, computer or FERRET data for missing *in situ* data.

4. Research questions

This study intends to addresses following research questions:

- How much is the variation between temperature logger data derived and the observed (*in situ*) from Icely weather station and also between Icely weather station data and windguru data?
- How to replace missing values in the Sagres weather station data?
- Which of the two datasets (i.e Windguru and temperature logger data) is better for use to substitute the missing data to effectively assist in identifying upwelling events?
- Which methods and software used to achieve this?

5. . Materials and Methodology

Software's used in this study include; Microsoft Office Excel 2003, SYSTAT v10, Matlab, FERRET v5.51 and Climate Predictability Tool v10.03 (CPT).

5.1. Data Management and description

The datasets comprises of: Daily temperatures, wind direction and speed, and this was obtained from Dr.Icely Weather station, at Surges records air temperature, a temperature logger attached to a signal buoy for offshore aquaculture, and this measures Sea surface temperature (SST) and the windguru dataset obtained from the website archive *(*www.windguru.cz), this also measure SST . These datasets, span from August to October 2009, and on daily basis. There is SST data for August 1999 from the temperature logger and this will compared with the historical Ferret mean SST for August (1946-1989). The other set of data is from the Meteorological weather station at Sagres has a lot of missing values and it is for the year 1999, and this is mainly wind

direction and speed on daily basis. This dataset is to be compared with the derived surface wind from NASA satellites by using FERRET software. There are three techniques used in this study to determine which of the dataset can best be used to replace missing values especial on the Sea surface Temperature datasets. The approaches are:

1. Plotting the daily temperature datasets in Lines on 2Axes and deturmining their skills using microsoft Excel and SYSTAT repectively.

2. Principal component regression analysis using satellite data in Climate Predictability Tool (CPT) Software;

3. Comparison with the Ferret software.

5.2.First Approach

Plotting the daily temperature datasets in Lines on 2Axes and deturmining their skills using microsoft Excel and SYSTAT repectively. Daily temperature data as well as wind direction and speed were analyzed using Excel. This was the initial data which was selected. This was done by listing the two data sets in column side by side. The first column represented date and time, the second column was for Automatic station data that is temperature logger data, the third column is the Icely weather station data and the third represents the windguru temperature data as in Table 1. From the Tables 1, 2 and 3 at the appendix C, the Icely weather station has some missing data, which needs to be replaced. SYSTAT is used to determine the skill which helps to know how the two data sets are close to each other. The software draws the histograms as well as the scatter diagrams.

5.3.SecondApproach

Replacing missing values using satellite estimates in CPT requires downloading the monthly satellite grid point data of the months one wishes to have some replacement. Note that each month needs to be handled separately, therefore you have to change the time frame to suit the name of the month you wish to download. So it may be better to download the satellite data in separate monthly files. This applicable for missing values of monthly datasets. The method used is the Principal Components Regression (PCR).The first thing is to know the boundary limits of the country or region to work on, in terms of coordinates (locations). For the Portugal coastline (Sagres) for example the locations are as follows i.e. 2°x2° apart: longitudes: 37ºN, 39ºN, 41ºN, 43ºN and latitudes: 009ºW, 011ºW, 013ºW, 015ºW. Then, the downloaded data is cut to suit the locations accordingly. The blank spaces are replaced with –999 before you run CPT as in (Table.4),at Appendix C. The first row is for stations names merged with satellite grid numbers. Second row is for Latitude, third row is for Longitude and the rest is the years and data. This is repeated for each month.

The missing values option to replace missing data is set using the nearest neighbour.For cases where there are a lot of missing values; Random numbers is the best see Fig. 4.

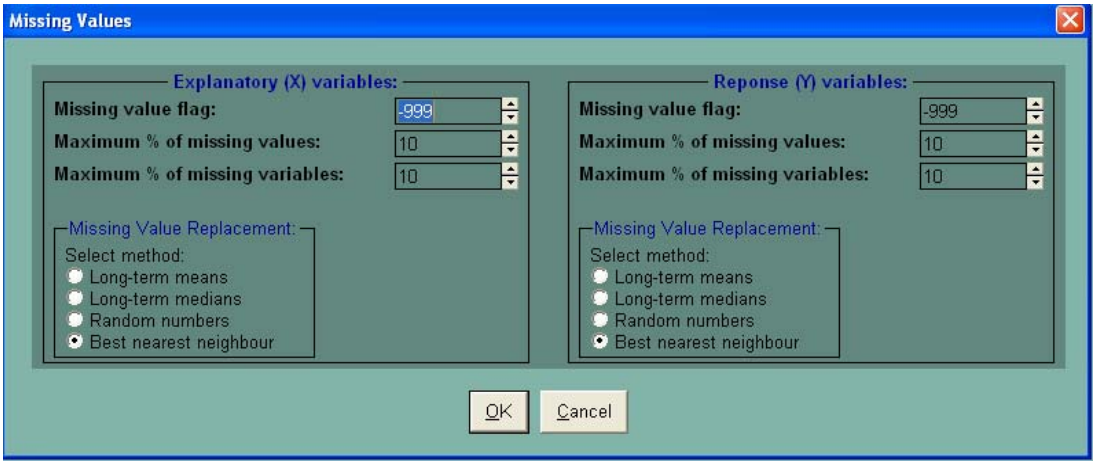

Fig.4. CPT window for determining Missing values, with the Best nearest neighbour option selected.

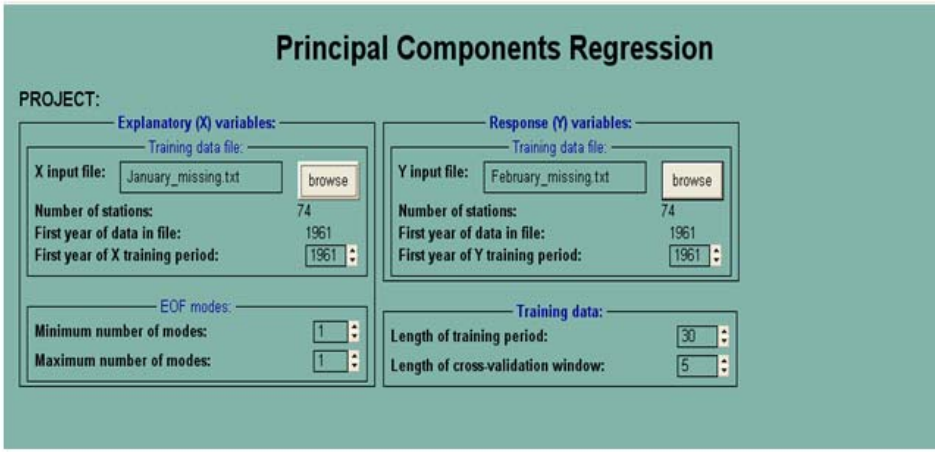

Fig.5. CPT Window to run the Principal Components Regression to replace the missing values for the months.

In CPT you have to put the January file as X dataset and the February File as a Y dataset. When running the inputs in CPT, they have to be in pairs as in Fig.5. Run CPT and save the input files using File –Data Output. After CPT has run, the filled file can be opened in Microsoft Excel (Table 5) at Appendix C.

5.4.Third approach

FERRET software is the main tool used in this study and can be used also to assist in filling the missing data by plotting the data and compare with the observed data for a particular day or month. In this study, derived daily surface winds at midday for August 1999 are plotted and compared as well as used where missing values are on the Sagres Meteorological data for August 1999 as well. This is an analysis tool for gridded data.

FERRET is an interactive computer visualization and analysis environment designed to meet the needs of oceanographers and meteorologists analyzing large and complex gridded data sets. “Gridded data sets” in the FERRET environment may be multi-dimensional model outputs, gridded data products (e.g., climatologies), singly dimensioned arrays such as time series and profiles, and for certain classes of analysis, scattered n-tuples (optionally, grid-able using FERRET’s objective analysis

procedures). FERRET accepts data from ASCII and binary files and from two standardized, self-describing formats. FERRET's gridded variables can be one to four dimensions usually (but not necessarily) longitude, latitude, depth, and time. The coordinates along each axis may be regularly or irregularly spaced.

FERRET offers the ability to define new variables interactively as mathematical expressions involving data set variables and abstract coordinates. Calculations may be applied over arbitrarily shaped regions. Ferret's "external functions" framework allows external code written in FORTRAN, C, or C++ to merge seamlessly into FERRET at runtime. Using external functions, users may easily add specialized model diagnostics, advanced mathematical capabilities, and custom output formats to Ferret. A collection of general utility external functions is included with FERRET (Hankin and Denham, 1996).

FERRET provides fully documented graphics, data listings, or extractions of data to files with a single command. Without leaving the Ferret environment, graphical output may be customized to produce publication-ready graphics. Graphic representations include line plots, scatter plots, line contours, filled contours, rasters, vector arrows, polygonal regions and 3D wire frames.Graphics may be presented on a wide variety of map projections. Interfaces to integrate with 3D and animation applications, such as Vis5D and XDataSlices are also provided.Ferret has an optional point-and-click graphical user interface (GUI). The GUI is fully integrated with FERRET's command line interface. The user may freely mix text-based commands with mouse actions (push buttons, etc.). FERRET's journal file will log all of the actions performed during a session such that the entire session, including GUI inputs, can be replayed and edited at a later time.

Ferret was developed by the Thermal Modeling and Analysis Project (TMAP) at NOAA/PMEL in Seattle to analyze the outputs of its numerical ocean models and compare them with gridded, observational data. Model data sets are often multi-gigabyte in size with mixed 3- and 4-dimensional variables defined on staggered grids (Hankin and Denham, 1996).

Firstly, it is better to discuss how ferret works in plotting historical Meteorological parameters such as sea surface temperature (SST), air temperature (AIRT), Specific humidity (SPEH),Wind speed(WSPD), Zonal wind (UWND), Meridional wind (VWND) and Sea Level Pressure (SLP). This data is found in COADS climatologically data set using FERRET.COADS is the comprehensive ocean-atmosphere data set compiled from ship reports over the global ocean. The monthly climatology introduced here represents a simple average of all data available for each month of the year.(Hankin and Denham,1996).

6. Results and Discussion

Fig. 6 show two plots, the first one showing Icely Wx.station data versus windguru data (Fig.6A) and the second one shows Icely Wx.station data versus Temperature logger (Fig.6B) data plotted against time for the month of August. From Table 1 at the appendix C and from the graph below, it is clearly that the Icely weather station temperature data was missing at the beginning of the month up to 17th August and has highest values as compared to the other two datasets that is the Temperature logger data from the sensors in the ocean and the Windguru dataset. This is basically because it is outside the ocean on the land. It must be pointed out that land heats faster than the ocean and consequently, loses heat faster than the oceans. The mean difference between the Icely Wx.data and the other two automatic station data is about 1.7˚C,but in some cases like on 28-08-2009 the difference was 0.1˚C ,and on 25-08-2009 it was less than

0˚C i.e. at -0.1˚C. The windguru curve seems to follow the observed Icely Wx. data pattern. It must be pointed out that the Icely weather station Data measures Air temperature while the other two records SSTs.

A

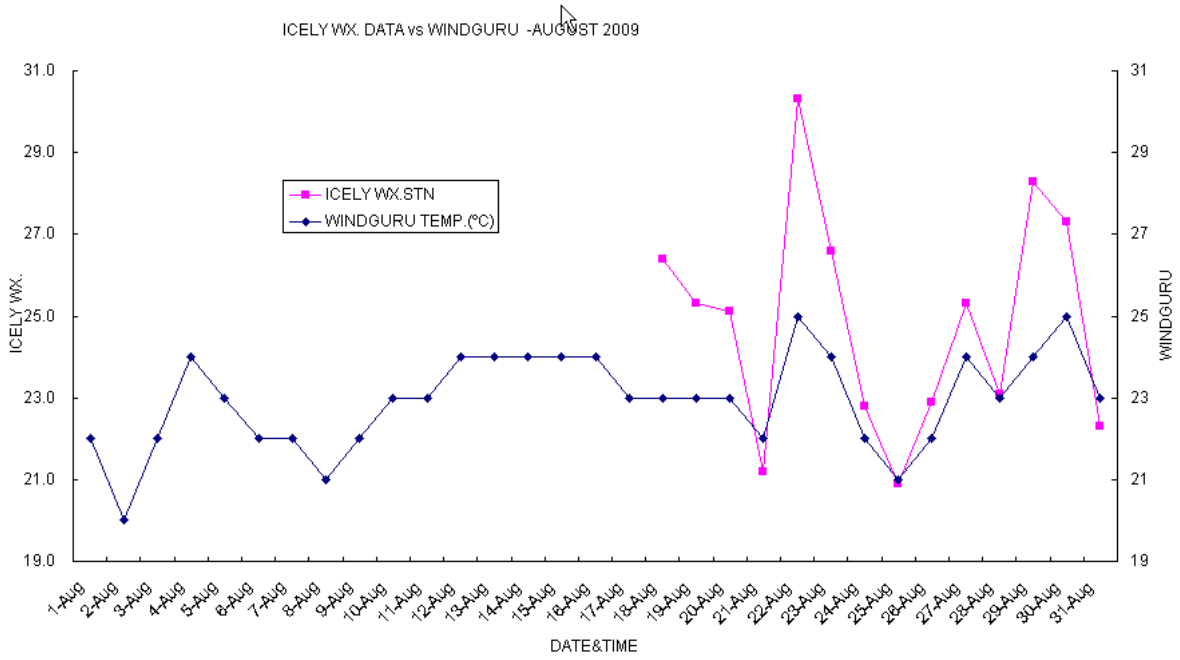

B

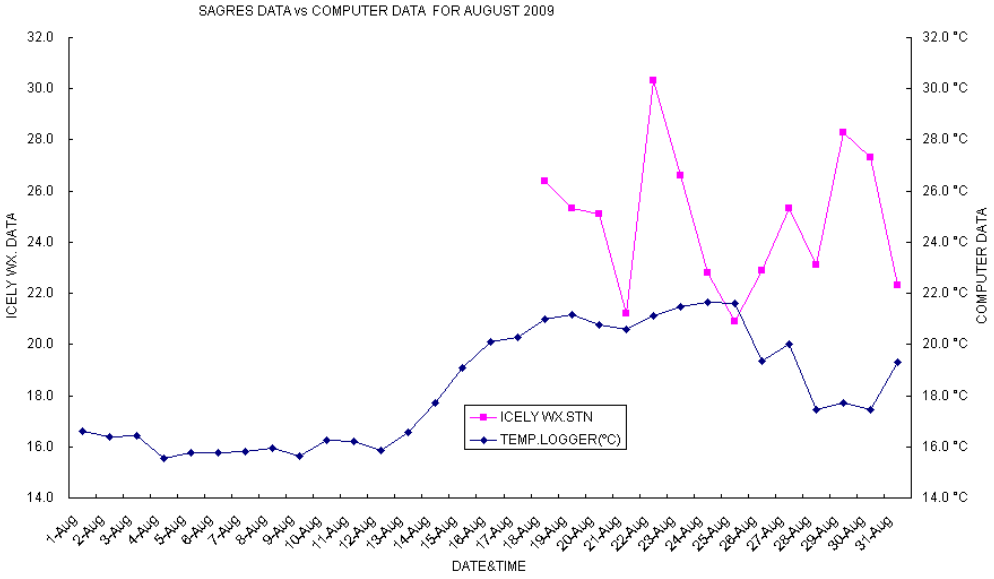

Fig.6. plot of temperatures Icely Wx. (Sagres) versus windguru data (A) and Icely Wx. Vs Temperature logger (B)for August 2009.

Fig .7.below show the skill of the relationship of temperature datasets between the Icely weather station data at Icely Wx. Station and Windguru as well as Icely Wx. Station and temperature logger .The skill between the Sagres temperature data windguru temperature is 88% and for Sagres and temperature logger data was -14%.

	ICELY	WINDGURU
ICELY	1.000	
WINDGURU	0.879	1.000

	ICELY	LOGGER
ICELY	1.000	
LOGGER	-0.136	1.000

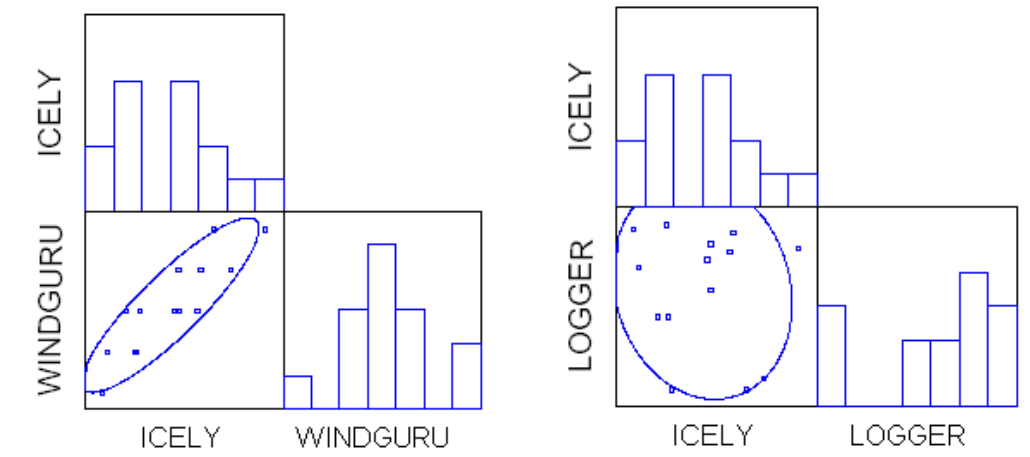

Fig.7.Showing the skills between Icely Wx data at Sagres and the Windguru (88%) Left, and Temperature logger(-14%) Right, temperature datasets for August 2009.

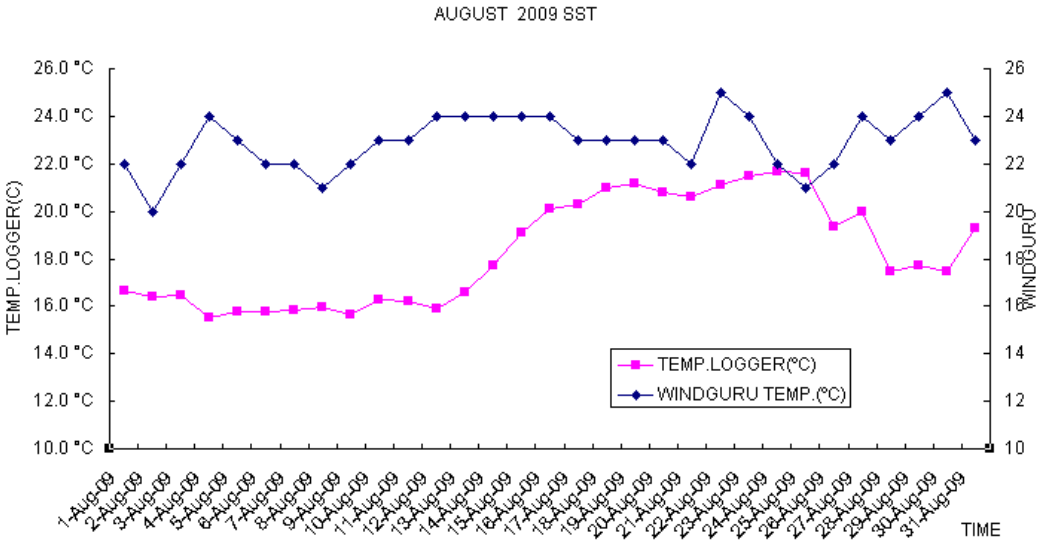

Fig.8. plot of Sea temperatures windguru data Vs Temperature logger for August 2009.

	WINDGURU	LOGGER
WINDGURU	1.000	
LOGGER	-0.364	1.000

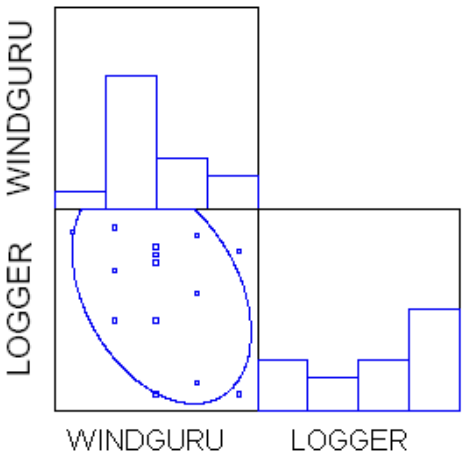

Fig.9.Showing the skills between Windguru (-36%) and Temperature logger sea temperature datasets for August 2009.

From the plots of windguru and Temperature logger Fig.8 and 9,the skill is(-36%),implying that the skill is very low between the two datasets.

The September plots in Fig.10. has almost complete data and the difference here among the three datasets is 0.97˚C as the mean correction so to say. There some times when the temperatures coincided like on 24-09-2009 the temperature was 23˚C for both windguru data and Icely Wx.data.

A

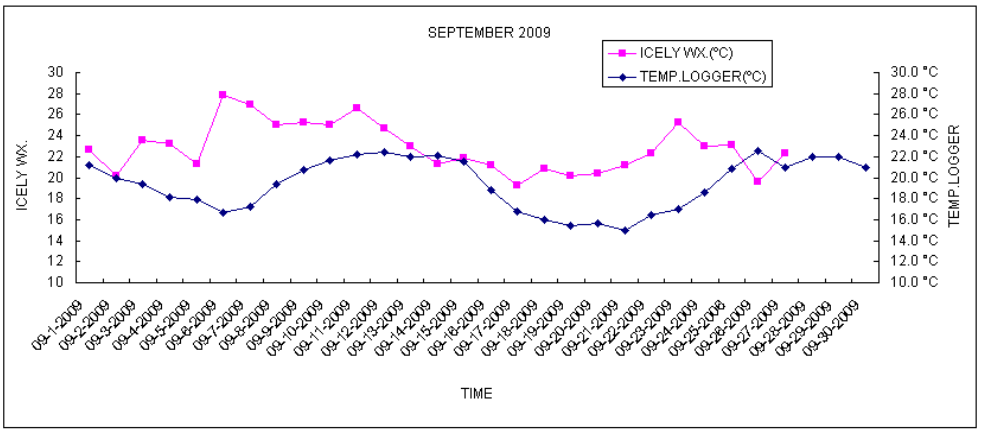

B

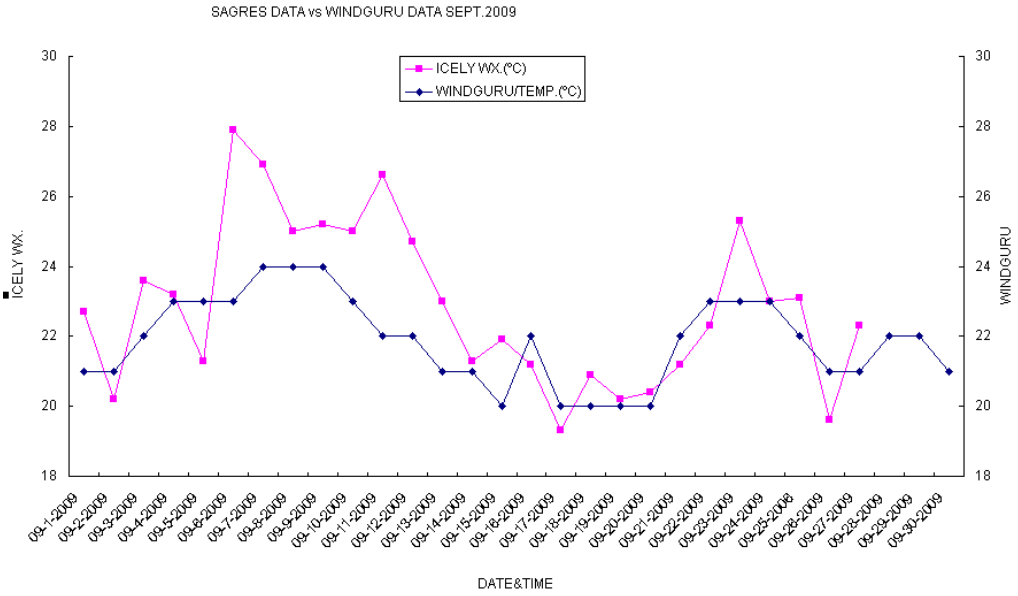

Fig 10. Plot of temperatures of Icely Wx. Stn. versus Temperature logger (A) and Icely Wx. Stn. Vs windguru data (B) for September 2009.

The skills for the September 2009 were as follows: Icely Wx.stn. temperature and windguru 71% ,while Icely Wx.stn and Temperature logger 16% (Fig.11.) below.

	ICELY	WINDGURU
ICELY	1.000	
WINDGURU	0.712	1.000

	ICELY	LOGGER
ICELY	1.000	
LOGGER	0.163	1.000

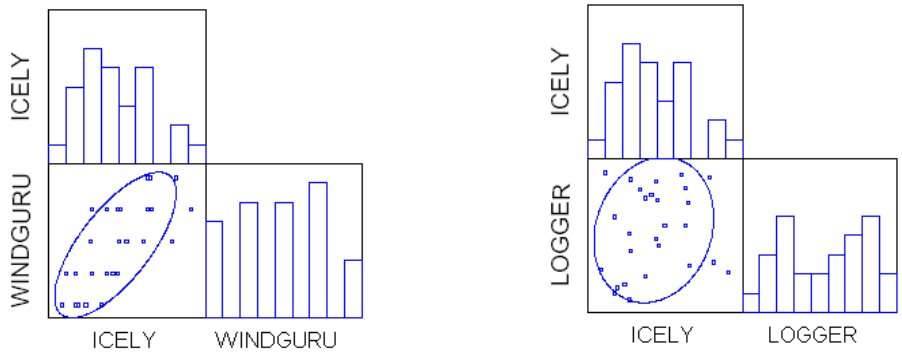

Fig.11. Showing the skills between Icely Wx. Stn. and the Windguru (71%) Left and Temperature logger (16%)Right, temperature datasets for September 2009.

The windguru and the Temperature logger were in agreement throughout. The mean correction here is at 0.6˚C.

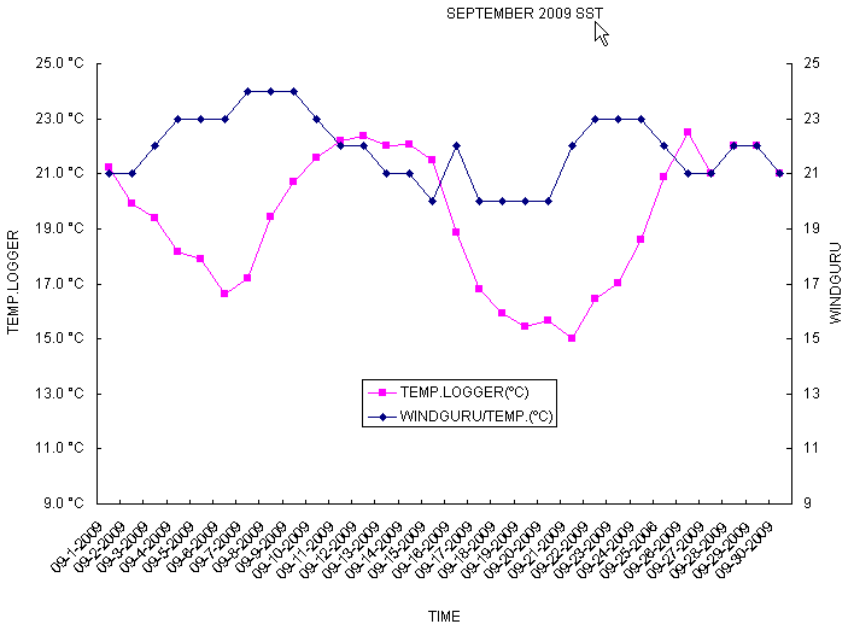

Fig12. Plot of Sea temperatures windguru data Vs Temperature logger for September 2009.

	LOGGER	WINDGURU
LOGGER	1.000	
WINDGURU	-0.012	1.000

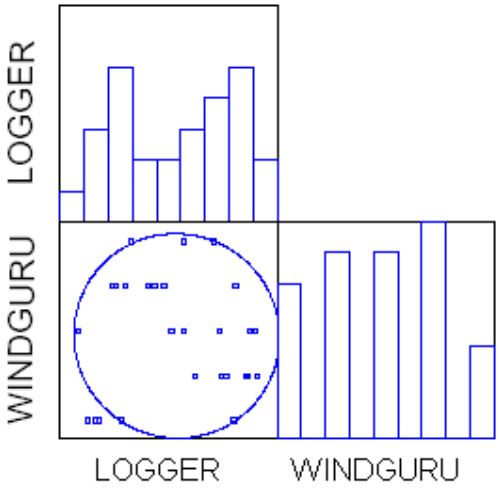

Fig.13. Showing the skills between the Windguru (-01%) and Temperature logger for September 2009.

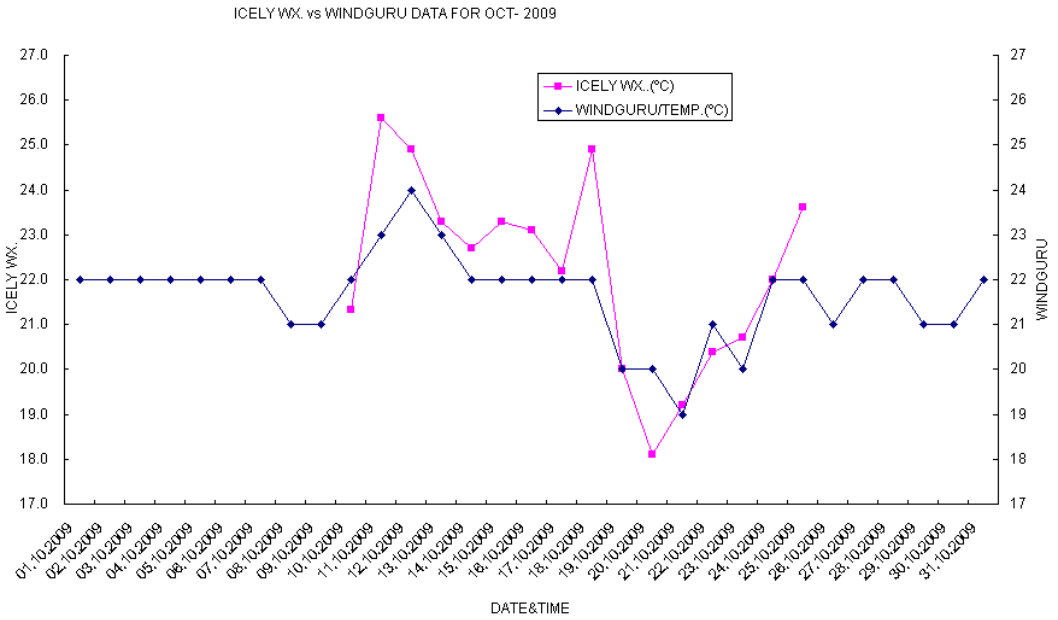

Fig14. Plot of temperatures of Icely Wx.) versus windguru data for October 2009

Similarly the plots for the October 2009, (fig.14), the trend is that as the Icely Wx. was going up and so was the windguru. The October data was only for windguru and the Icely Wx.data. The data for Temperature logger was not available and also the Icely Wx.data was missing at the beginning of the month up to October the 9th . The skill here is at 87% (Fig.15).

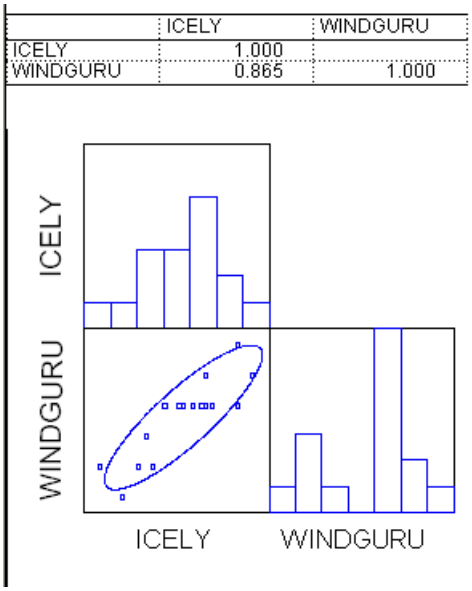

Fig.15. Showing the skill(87 Icely Wx. and the Windguru datasets for October 2009.

A comparison of the environmental data demonstrates that amongst August, September and October 2009, the windguru data was more in agreement with the other two datasets and the trend favored the Icely Wx. temperature as the Icely temperature was going up or down and so was the windguru see temperature data on the plots and also the skills were higher. Fig.6A, 7, 10B, 11, 14 and 15.

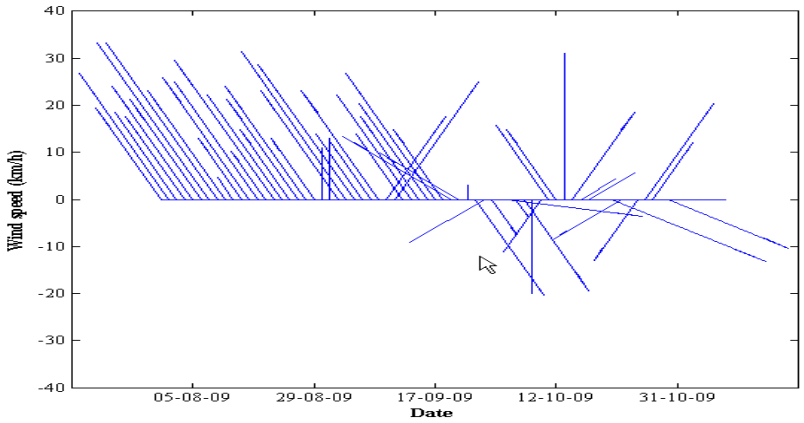

Fig.16. Wind direction and Speed (represented by the length of line) for August to October 2009.

Figure 16 shows wind direction and speed for Icely Wx.stn. from August to October 2009.The graph was constructed using Matlab software and it was predominantly of northwesterlies (NW) with maximum velocity of 36km/h occurring consecutively on August 7 and 8th .2009. The wind plot (Fig.16), indicated that the wind speed was fluctuating rising and falling but generally inclined on the rising tendency, while the wind direction was steadily northwesterly flow.

This method was also used over Sagres by (Fragoso and Icely, 2009; Loureiro *et al.*, 2001). It is clear that the two days were upwelling periods because both the temperatures and wind regime was favorable for upwelling occurrences. The wind was

Northwesterlies and speed was high enough to effect the required Ekman transport.The temperature was 15.8˚C and 15.9˚C. respectively which is also within the specifications favourable for upwelling events.It can be noted that in the case of wind the variation is minimal as compared to the Icely weather station and the windguru. This can be confirmed by Fig.2, showing the historical three monthly averages of the Portugal currents which are wind driven. The Temperature logger from the sensor in the water showed colder temperatures explaining upwelling events during the first week and again the whole of the third week, and this was also confirmed by the Northerly westerly winds (Fig.16 and 17), with higher wind speed in the first week reaching as strong as 37km/h and so forth.

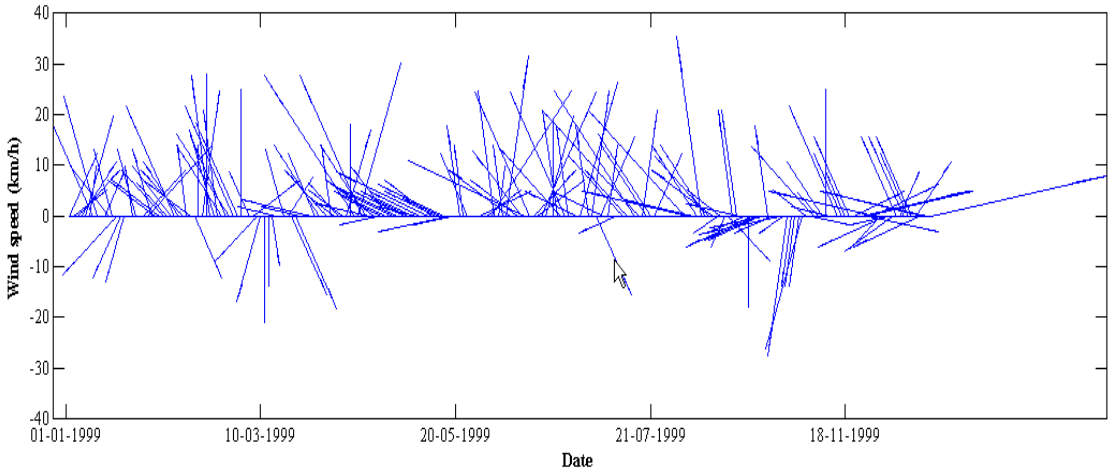

Fig.17. Wind direction and Speed (represented by the length of line) for 1999.

Fig.17. shows the plot of wind direction and speed for 1999 using Matlab software as well.The maximum velocity recorded during this period was 46km/h on 30th December 1999 and the wind direction was Northeasterlies, the temperature was 14.5˚C.The second higher velocities were recorded in the main upwelling month of August on 20th with 36km/h and the direction of North –northwesterlies (NNW) with temperature of

14.5˚C as well of and also in April the 13th at 36km/h and wind direction of Northwesterlies (NW) with 16˚C. On 1st August the velocity was at 32km/h and the direction was NW, with temperature of 14.5˚C. Similarly in this period, the main wind regime is Northwesterly component as in fig.2.This indicates that even in the case of wind, the windguru data is consistent with istu data at Sagres weather station.

The coads-climatology in Ferret contain the data variables shown in Table 6 at Appendix C.The monthly climatology introduced represent a simple average of all data available for each month of the year from 1946-1989.

In these data sets the index "I" refers to longitude, "J" to latitude, "K" to the vertical dimension, and "L" to time. In the listing the values under each qualifier present the points available along that axis. For example 1:180 indicates that locations 1 through 180 are represented in the data set."L" refers to time in months i.e. 1:12 means January to December. Therefore if one wants to plot SST and winds for the months of January along and off the Portugal coast, in Ferret you use the following commands:

After setting and showing the data as in table 6 at Appendix C, the next step is to set the region say:

```
yes? SET REGION/Y=30N:50N/X=30W:4W
yes? SHADE/L=1  SST
yes?  GO land red
yes? VECTOR/OVERLAY/L=1  UWND,VWND
```

The above commands will give rise to in examples as in Fig.14,15and 16 below.Note that Y represents the longitude of the required region in this case and X is the latitude.

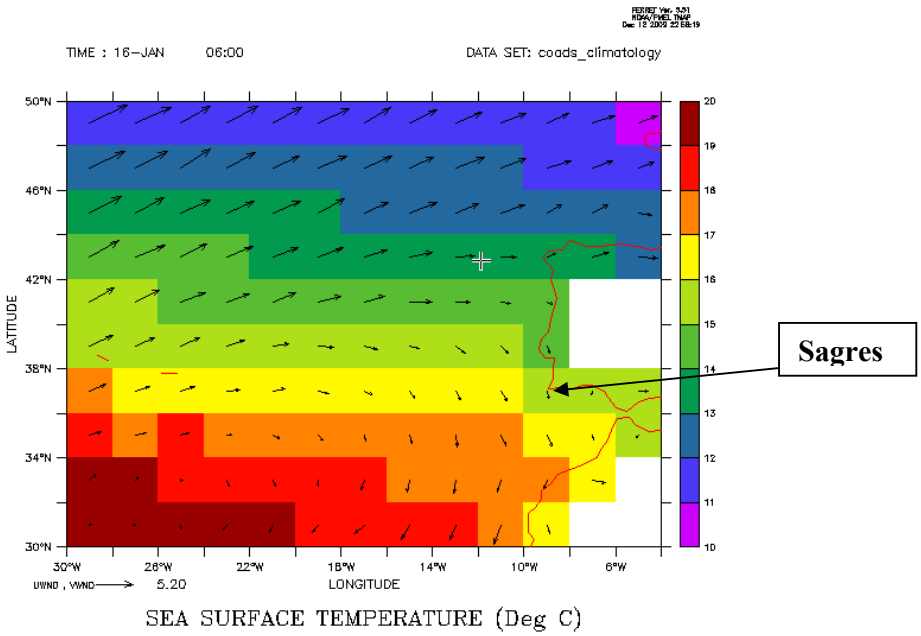

Fig.18. Analysis of sea surface Temperature with wind direction and speed for the month of January (1946-1989)overlaid using FERRET.

To draw the winds only, go to VECTOR/L=1 UWND,VWND and get Fig.19. below:

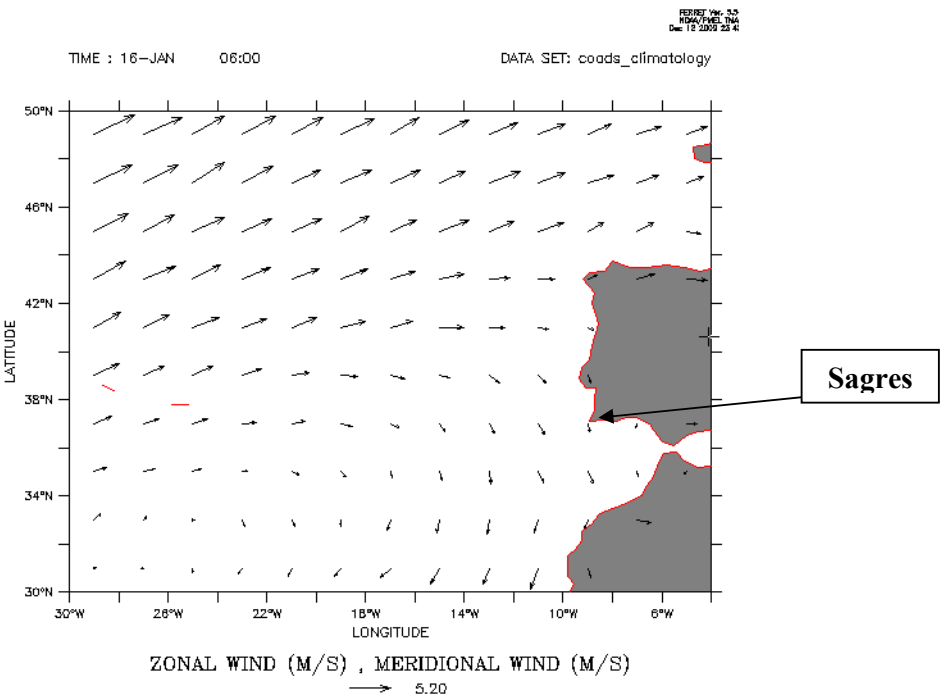

Fig.19. Example for the January (1946-1989) winds, plotted by FERRET.

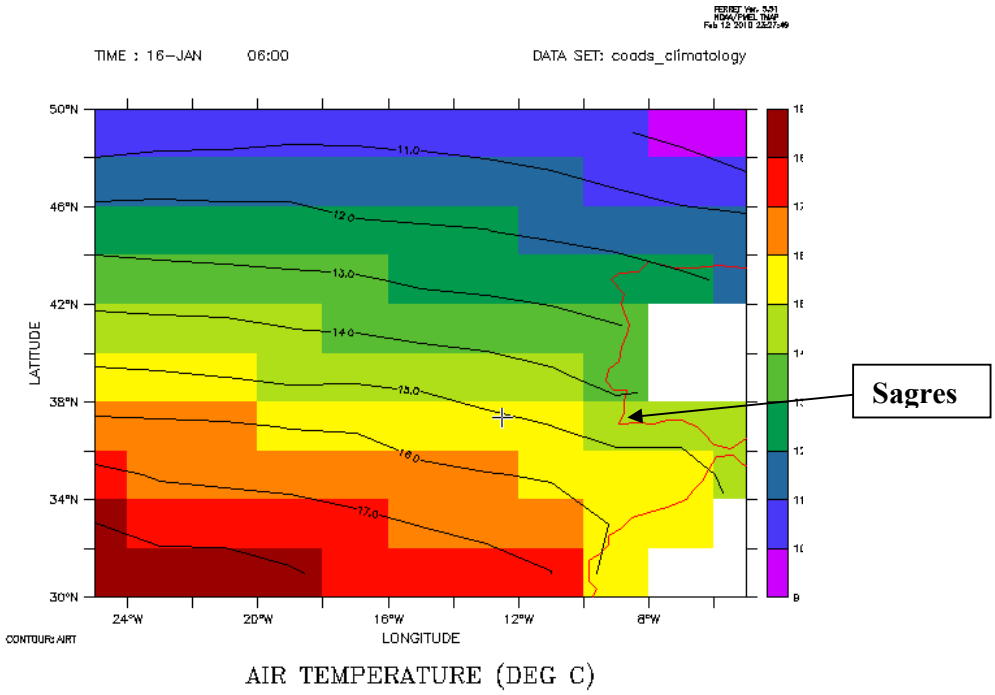

Fig.20. Example for the January (1946-1989) Air temperatures with contours overlaid using FERRET**.**

The contours for the temperature or wind direction can be overlaid on the shaded plot by using the command 'COTOUR /OVERLAY/L=1 AIRT and this gives the plot as in Fig.20 above.

Table 8 at the Appendix C. Shows the Wind speed and direction for Meteorological station at Sagres and this was compared with the Ferret surface wind plots so as can be substituted where missing values as in the examples below: On 20th August 1999 at 12:00 hrs, the wind direction was 350˚ which was NNW and the speed in meters /second was 10m/s (Table 10 at the Appendix C). A comparison with FERRET plot of the same in time and date are agreement as can be noticed on the plots below (Fig. 21 and 22 respectively).

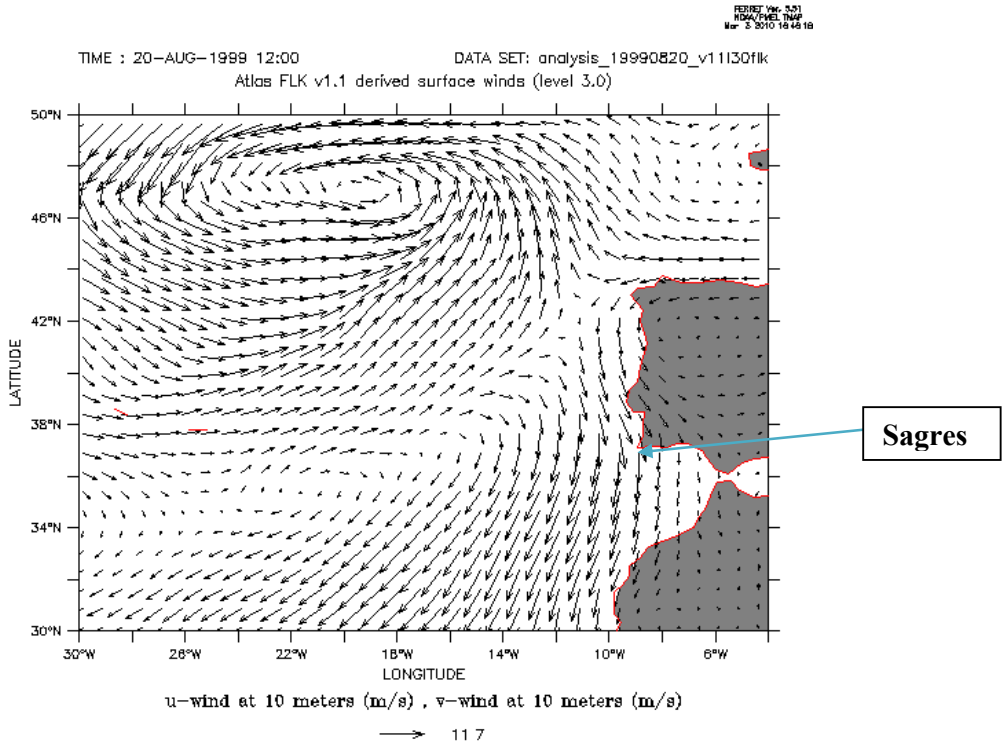

Fig.21. FERRET surface Winds for 20th August 1999,in vector formart.

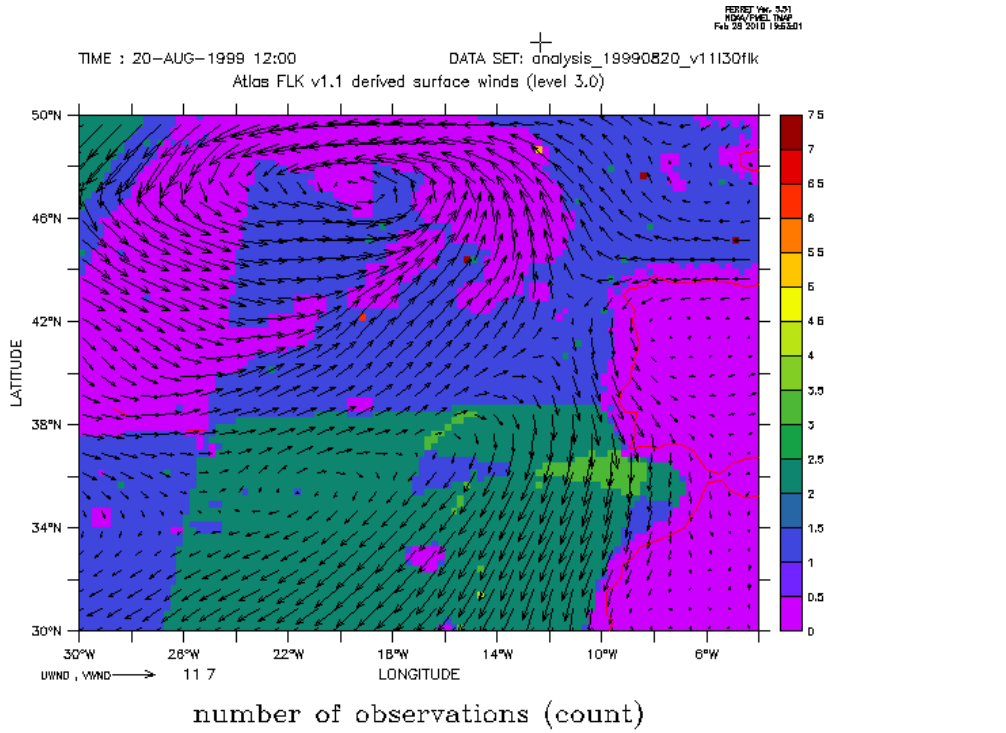

Fig.22. Ferret surface Winds for 20th August 1999,in vector format overlaid on number of observations(count)

N.B the arrow UWND,VWND ⟶ 11.7 as indicated represent the speed of 11.7m/s as indicated on both figures and the direction of the wind is indicated by the arrow and is NNW wind (i.e 350˚ and 10m/s as in Table 10).

Another example are on 19 and 21st August, 1999, where the data was missing and Ferret can be used to substitute those missing values as shown on Fig.23 and 24 below respectively.

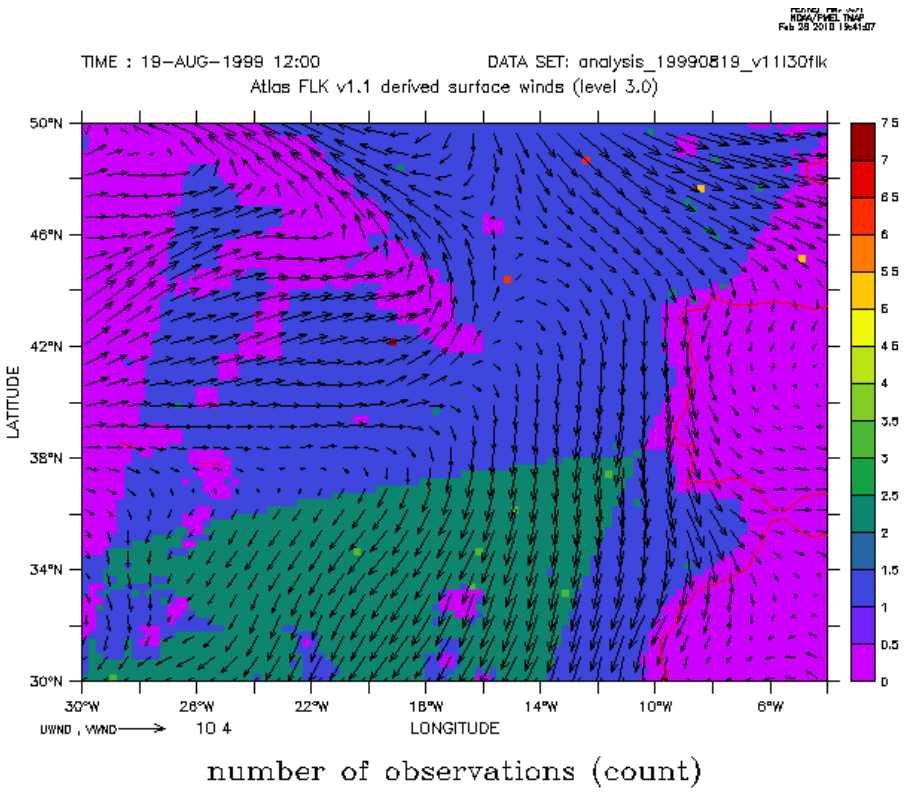

Fig.23 Ferret surface Winds for 19th August 1999,in vector formart overlaid on number of observations(count)

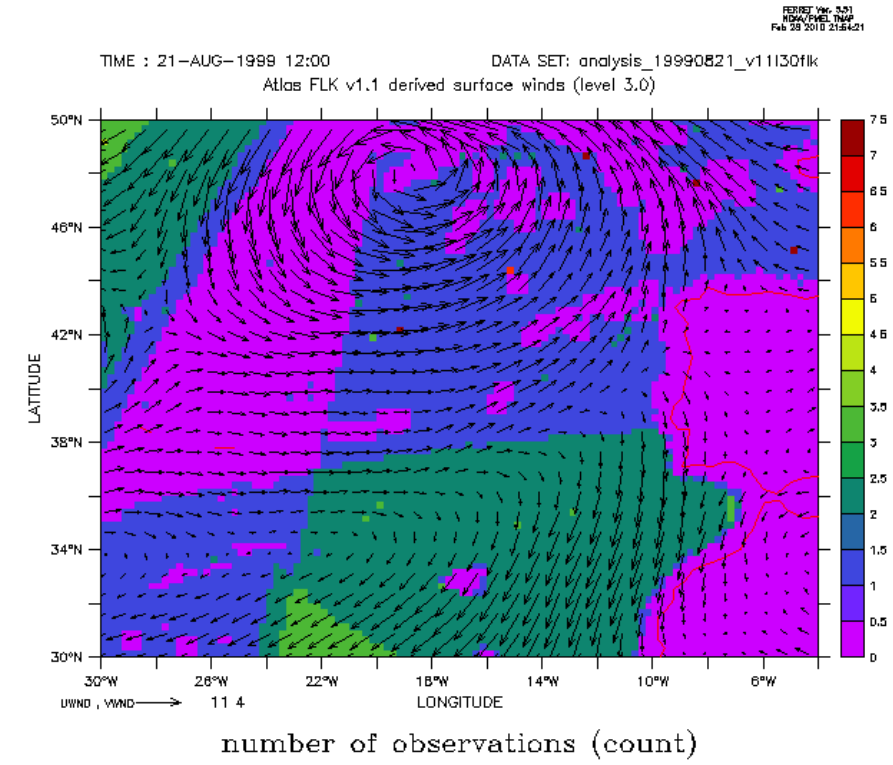

Fig.24. Ferret surface Winds for 21st August 1999,in vector formart overlaid on number of observations(count)

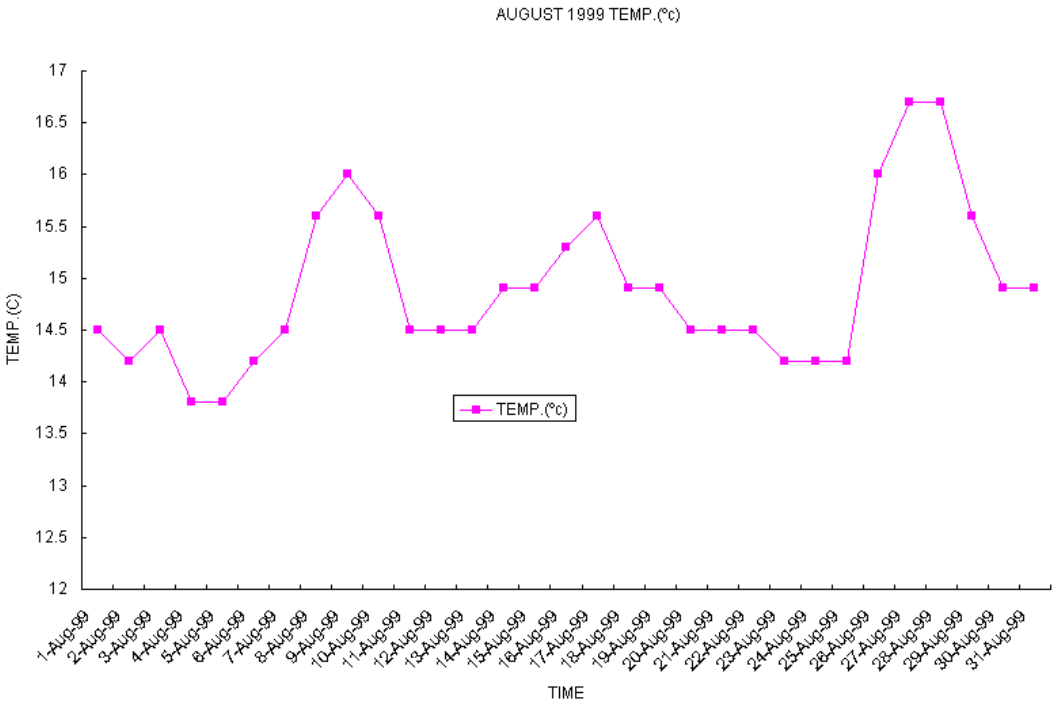

Fig.25. August 1999 temperature logger daily sea Temperatures

Fig 25. Show the August sea temperature from the temperature logger at Sagres.The temperature was between 13˚ to 17˚C,which was favarable for upwelling.

Deductions from Fig.21,22, 23, 24 and 25 is that wind regime together with that at Sagres favor upwelling as evidenced from the wind to the north of the Sagres coast is divergent implying that water was moving apart which is one of the mechanism that causes upwelling.

A comparison of the environmental data demonstrates that between May and September the strong fluctuations in sea surface temperature (SST) are related to wind events with lower temperatures occurring after periods of dominant north-westerly winds. Similar observations have been made for this region in previous studies (e.g. Fiúza, 1983; Loureiro *et al.*, 2005). The comparisons done by other studies, evidence that the Sagres winds are spatially more confined and exhibit a stronger spatial heterogeneity than the winds at Sines. The zone of maximum correlation extends concentrically around Cape St. Vincent (Sãnchez *et al.*, 2007).

7. Conclusions

The skill tests between the Icely Wx.stn air temperature data and Windguru as well as temperature logger indicate that the Windguru data is a good substitute of missing values on the Icely Wx.stn (*in situ* data) as well as the Meteorological weather data because it showed very high skill as compared to the temperature logger data. Besides, has the same trend with Icely Wx.stn.temperature, as the Icely temperature data was going up or down, and so was the Windguru data on the plots. Comparison between windguru and temperature logger, proved that the two dataset are not related as can be deduced from the very low negative skills.

The Ferret analysis has proved also to be a good tool for making substitution to the missing Meteorological data as evidenced by the daily comparisons with the August1999 Ferret derived surface winds and Meteorological wind dataset for Sagres.

There is classical view that in this region favourable winds force near-surface offshore transport and coherent flow along the coast, does not apply throughout the upwelling season (Relvas and Barton,2005). Other methods may still be utilized where the Ferret tool fails to meet the expectation, this in the case of non-availability of data for the Ferret software. These considerations can alleviate the difficulties in explaining the biological and chemical process that take place along the Sagres coastline such as upwelling events.

8.References

Bischof, B., Mariano, A. J., Ryan. E.H. (2003). "The Portugal Current System." Ocean Surface Currents (http://oceancurrents.rsmas.miami.edu/atlantic/portugal.html)

Barton, E. (2001). Canary and Portugal currents. University of Wales, Bangor, UK. Copyright Academic Press doi:10.1006/rwos.2001.0360.

Bettencourt, A. M., Bricker, S. B., Ferreira, J.G., Franco. A., Marques, J.C., Melo, J.J., Nobre, A., Ramos, L., Reis,C.S., Salas, F., Silva, M.C., Simas, T., Wolff W.J.(2004).Typology and Reference conditions for Portuguese Transitional and Coastal Waters, Development of Guidelines for the Application of the European Union Water Framework Directive, INAG and IMAR, Lisbon, Portugal. 98p.

Brogueira M. J., Cabeçadas G., Gonçalves C. (2004) Chemical resolution of a meddy emerging off southern Portugal, Continental Shelf Research. 24**:** 1651-1657. ISSN 0278-4343

Conway, E. D. (1997). An introduction to satellite image interpretation, Johns Hopkins Univ. Pr. Maryland Space Grant Consortium, The Johns Hopkins University Press, Baltimore, 242 p. ISBN 0 8018 5576 4.

Detlefsen, H. and P. Speth.(1980). Investigations on coastal upwelling off Northwest Africa and Portugal with empirical orthogonal functions, Journal Ocean Dynamics. 33**:** 210-221.

Fiúza,A.F.G.,M.E. Macedo and M.R. Guerreiro,(1982). Climatological space and time Variation of the Portuguese coastal upwelling. Oceanol.Acta, 5(1): 31-40

Fiúza, A.F.G., 1983. Upwelling patterns off Portugal. In: Suess, E., Thiede, J. (Eds.), Coastal Upwelling: its Sedimentary Record. Part A. Responses of the Sedimentary Regime to Present Coast Upwelling. Plenum, New York, 85–98 p.

Fragoso, B. and J. D. Icely (2009). Upwelling Events and Recruitment Patterns of the Major Fouling Species on Coastal Aquaculture (Sagres, Portugal). Journal of Coastal Research,SI 56 (Proceedings of the 10th International Coastal Symposium),419-423.Lisbon,Portugal,ISSN 0749-0258.

Hankin, S and Denham, M (1996). FERRET User's guide, NOAA/PMEL/TMAP (1996) Version 4.4.

Harimoto, T., Ishizaka, J., Tsuda, R.(1999).Latitudinal and vertical distributions of phytoplankton absorption spectra in the central North Pacific during spring 1994,. Journal of Oceanography, Volume 55, Number 6, December 1999 , 667-679(13) pp.

Loureiro, S., Newton, A., Icely, J.D.(2001). Microplankton composition, production and upwelling dynamics in Sagres (SW Portugal) during the summer of 2001.Scientia Marina, 69. 323-341.

Loureiro, S., Newton, A, Icely, J.D. (2005). Microplankton composition, production and upwelling dynamics in Sagres (SW Portugal) during summer of 2001. Scientia Marina, 69. 323-341.

Loureiro, S., Icely, J.D., Newton, A. (2008). Enrichment experiments and primary production at Sagres (SW Portugal), Journal of Experimental Biology and Ecology, 359, 119-125.

Martins, C. S.,Hamann,M.,Fiúza,A.F.G.(2002). Surface circulation in the eastern North Atlantic, from drifters and altimetry, Journal of Geophysical Research**,** 107, 3217, doi: 10.1029/2000JC000345**.**

Peliz, A. J.,Fiúza, A. F. G.Za. (2001). Temporal and spatial variability of CZCS-derived phytoplankton pigment concentrations off the western Iberian Peninsula. International Journal of Remote sensing 7,1363-1403.

Perez, Fiúza F., C. G. Castro, X. A. Alvaréz-Salgado, A. F. Rios (2001). Coupling between the Iberian basin-scale circulation and the Portugal boundary current system: a chemical study, Deep-Sea Research I, 48, 1519-1533.

Relvas, P., Barton, E.D. (2002). Mesoscale patterns in the Cape São Vicente (Iberian Peninsula). Journal of Geophysics Research. 107, 3164, doi: 10.1029/2000JC000456.

Relvas,P., Barton, E.D., Dubert,J., Oliveira,P.B., Peliz, Da Silva,J.C.B.,Santos, A.M.P. (2007). Physical oceanography of the western Iberia ecosystem: Latest views and challenges, Progress in Oceanography Vol.74: 149–173.

Sãnchez, R. F., Relvas, P. ,Pires,H.O. (2007). Comparisons of ocean scatterometer and anemometer winds off the southwestern Iberian Peninsula, Cont Shelf Res 27:155–175.

Santos, A. M. P, de Fátima Borges, M.; Groom,S. (2001). Sardine and horse mackerel recruitment and upwelling off Portugal. Fisheries Research, Vol. 58: 589. Instituto de Investigação das Pescas**.**

Solignac, S.,de Vernal, A.,Giraudeau,J. (2008). Comparison of coccolith and dinocyst assemblages in the northern North Atlantic: How well do they relate with surface hydrography?, Marine Micropaleontology, 68, 115-135.

Sousa, F. M. and A. Bricaud, (1992). Satellite-derived phytoplankton pigment structures in the Portuguese upwelling area, Journal of Geophysical Research 97, 11343-11356.

Villa, H., Quintela, J., Coelho, M.L., Icely, J.D., Andrade,J.P. (1997). Phytoplankton biomass and zooplankton abundance on the south coast of Portugal (Sagres), with special reference to spawning of Loligo vulgaris. Scientia Marina. 61**:** 123-129.

Wollast R. (1998). Evaluation and comparison of the global carbon cycle in the coastal zone and in the open ocean, In: The Sea: The Global Coastal Ocean: Processes and Methods. Brink, K.H. and A. R. Robinson, eds. Vol. 10. John Wiley & Sons, Inc. N.Y. 213-252 pp.

Wooster, W.S., Bakun, A., McLain, D.R., 1976. The seasonal upwelling cycle along the eastern boundary of the North Atlantic. J. Mar. Res. 34 (2), 131–141.

Appendix A. Review of Oceanographic and Meteorological Processes responsible for coastal upwelling.

1. Review

Global climate coupled ocean-atmospheric phenomena such as El Niño Southern Oscillation(Picaut *et al.,*1996),commonly known as El Niño / La Niña and the North Atlantic oscillation (NAO) plays an important role in the fluctuations of atmospheric processes. Sea Surface Temperature (SST) fluctuations of the tropical Eastern Pacific

Ocean occur in the case of El Niño Southern Oscillation (ENSO) and atmospheric pressure at sea-level difference between the Icelandic Low and the Azores High takes place during the North Atlantic Oscillation (NAO).

Upwelling of ocean water is affected by wind. As wind moves across the surface layer the water is dragged along due to frictional force and this top layer of water is pulled along in the same direction as the wind. Wind-driven upwelling systems are part of the coastal upwelling occurring along the Portuguese coastline, the western coasts of the Iberian Peninsula and Africa down to 15°N (Relvas and Barton,2002) Fig.1at Appendix B, shows the areas major upwelling in the world.

On an annual-mean basis, very warm surface water of about 29.8C occupies most of the area between 78N and 108S, 1308E and 1708W (Picaut *et al.*,1996), Fig.2. at Appendix B, Showing cold and warm water currents. Oceanography enables Oceanographers to forecast sea state in the same way that Meteorologists forecast the atmosphere today. Ocean state and wave height help the sailors to choose the best route, thus saving the valuable time.The distinct Pattern Of ocean-atmosphere relationship is associated with interdecadal variability in the North Atlantic region. The middle- and high-latitude sea surface temperatures (SST) display a long-term fluctuation with negative anomalies before 1920, and during the 1970s and 1980s. Positive SST conditions prevailed from about 1930 to 1960.(Kushnir, 1994).In the North Atlantic mid ocean area, an anomalous cyclonic circulation prevailed during years with warm SST, and an anticyclonic anomaly dominated during years with cold SST. These circulation anomalies are strongest during the winter months (Kushnir,1994).

Satellite infrared sensors only observe the temperature of the skin of the ocean rather than the bulk sea surface temperature (SST) traditionally measured from ships and buoys. In order to examine the differences and similarities between skin and bulk

temperatures, radiometric measurements of skin temperature were made in the North Atlantic Ocean from a research vessel along with coincident measurements of subsurface bulk temperatures, radiative fluxes, and meteorological variables. Recommendations were made to calibrate satellite derived SST's during night with buoy measurements and the additional aid of meteorological variables to properly handle temperature difference variations (Schluessel *et al.*,1990).

Chlorophyll patchiness caused by mesoscale upwelling at fronts were detected in the open North Atlantic during summer (Strass,1992). The mesoscale patches with highest chlorophyll concentrations occur at those sites where the hydrographic conditions are favorable for dynamic upwelling or where the distributions of the hydrographic variables indicate local upwelling events (Strass, 1992).

2.Global Climate-Coupled Ocean-atmospheric

The general circulation of the atmosphere imbeddes the hydrological cycle.Water balance at the surface and subsuface is strongly coupled with the patterns and behavior of the climatic system and the capability to simulate and predic the general circulation of the atmospheric fluid is thus of great importance to hydrology. Climatic general circulation models (GCMs) have been devised to produce the basic patterns and processes in the atmospheric system (Entekhabi, 1990).

2.1. El Niño Southern Oscillation (ENSO)

The El Niño Southern Oscillation (ENSO) represents the largest signal in inter-annual climate variation, affecting global atmospheric and oceanic circulation patterns. The phenomenon undergoes cycles between warm ENSO conditions (which are extreme during El Niño episodes) and cold ENSO conditions (extreme during La Nina episodes) (Viboud *et al.*, 2004). Recent developments in the El Niño-Southern Oscillation

(ENSO) phenomenon have raised concerns about climate change. El Niño and La Niña are major temperature fluctuations in the tropical Pacific Ocean (see Fig.3), at Appendix B. They are Pacific signatures of the global ENSO phenomenon (El Niño-Southern Oscillation). Their effect on climate in the southern hemisphere is profound. Their role in global warming or cooling is an area of active research, with no clear consensus yet. Fig 4 at Appendix B.ENSO-Neutral conditions (a) compared to the warmer waters of a typical El Nino.

(b) Shown as sea surface temperature anomalies in the equatorial pacific ocean.

The atmospheric signature, the Southern Oscillation (SO) reflects the monthly or seasonal fluctuations in the air pressure difference between Tahiti and Darwin. Fig.5 at Appendix B.

2.1.1. El Niño Southern Oscillation (ENSO) Index

Fluctuations in tropical Pacific sea surface temperature (SST) are related to the occurrence of El Niño, during which the equatorial surface waters warm considerably from the International Date Line to the western coast of South America (Stenseth, *et al.*, 2003). However, it is important to remember that the pattern of relationship between SOI and rainfall (and temperature) can vary depending on the particular season and region. Additionally, the change in SOI over a specified period can be as important in understanding relationships between SOI and rainfall as is the absolute value in SOI. See fig.5. at Appendix B. Predictions of ENSO are done at International Prediction centers such as the IRI (International Research Institute for climate and society).Fig.6. at Appendix B and Table 9 at appendix C show ENSO probabilistic forecast for NINO3.4 Region.

2.1.2.El Niño

El Niño is an unusual warming of the ocean surface waters in the Eastern Pacific Ocean(Trenberth, 1997). This brings a lot of rains in other areas of the world and at the same time bring less rainfall or drought in other parts as well,in other words it can be reffered to as a circlic event. Fig.7 at Appendix B illustrates the above.

2.1.3. La Niña

La Niña is the name for the cold phase of ENSO, during which the cold pool in the eastern Pacific intensifies and the trade winds strengthen. The name La Niña originates from Spanish, meaning "the little girl", analogous to El Niño meaning "the little boy (Trenberth, 1997). La Niña is just the flipside of El Niño (Fig.7); La Niña tends to follow the El Niño. In 1997-1998, the biggest El Niño on record killed thousands of people (Ellison, 2009).

3. Ocean winds and circulation

Wind plays an important role in the air-sea interaction between sea surface temperature and upwelling. Wind regulates the temperature of seawater by transporting the heat across the water surface. The Sea Surface Temperature (SST) decreases at the beginning of the upwelling season, reaches its peak in May-June, corresponding with the winds, but starts rising in July due to increased solar heating at the surface, combined with the decreased alongshore winds in Central California (Diehl *et al.*,2007).

Trade winds are part of the atmospheric general circulations which drives the ocean currents (Fig.8 and Fig.9),at Appendix B, show the general circulation and wind effect on surface water currents respectively).Wind regulates the temperature of seawaters by

transporting heat across the water surface in form of land and sea breezes on a localized scale and through oceanic currents on large scale extent. Very high resolution radiometer (AVHRR) satellite images of sea surface temperature and time series of sea level height, wind velocities, and near shore sea surface temperature was studied and recorded at coastal sites within 200km of Cape São Vicente (Relvas and Barton,2002).

3.1.Ocean Surface Circulation

The westerlies are associated with heavy rainfall and thunderstorms in tropical Africa. The boundary between the northwesterly winds and the northeasterlies (northeast trade winds)is known as the Congo air boundary and it is associated with rainfall and thunderstorms. The convergence between the north east trade winds and the southeast trade winds is commonly known as the Inter Tropical Convergence Zone (ITCZ). The ITCZ is the main rain mechanism in most parts in the tropics. The trade winds (also called trades) are the prevailing pattern of easterly surface winds found in the tropics near the Earth's equator. The trade winds blow predominantly from the northeast in the Northern Hemisphere and from the southeast in the Southern Hemisphere. The trade winds act as the steering flow for tropical storms that form over the Atlantic, Pacific, and Indian Oceans that make landfall in North America, Southeast Asia, and India, respectively. Trade winds also steer African dust westward across the Atlantic ocean into the Caribbean sea, as well as portions of southeast North America.Fig.10, at Appendix B showing the trade winds as part of the Earth's atmospheric circulation. During an El Niño event, however, the trade winds weaken and the coastal upwelling diminishes, (Conway, 1997).

The NAO is a large scale seesaw in atmospheric mass between the subtropical high and the polar low. The corresponding index varies from year to year, but also exhibits a

tendency to remain in one phase for intervals lasting several years.(Hurrell *et al.*, 2003).The surface ocean currents circulations are powered by the prevailing winds. The forces that drive and direct the movement of the oceanic currents are: Wind, Coriolis force, Gravity and Friction .The circulations in the Northern Hemisphere are clockwise while in the southern Hemisphere is anticlockwise see Fig.11, at Appendix B. It is suspected that global warming might have a significant effect on the currents; see Fig.11 for details.

4. Northern Atlantic Winds

Wind circulation over the northern Atlantic ocean is associated with northern Atlantic upwelling system of western coast of the Iberian Peninsula (Peliz *et al.*, 2002) and the coastal upwelling region near Cape São Vicente (Relvas and Barton,2002).

In the Northern Atlantic, as the Gulf Stream flows north, it encounters the Labrador flowing south along the banks of Cape Hatteras. As these two currents meet, they begin to meander (they wind back and forth like a snake). Eventually, these meanders "pinch off" from the main flow and become independently rotating structures, known as rings.(see Fig.12 at Appendix B).These are the warm core rings and the cold core rings, previously known as eddies.

4.1. Northern Atlantic Oscillation (NAO)

This north Atlantic circulation is known as “The North Atlantic oscillation (NAO)”.This is a climatic phenomenon in the North Atlantic Ocean of fluctuations in the difference ofatmospheric pressure at sea-level between the Icelandic Low and the Azores high. Through east-west oscillation motions of the Icelandic Low and the Azores high, it controls the strength and direction of westerly winds and storm tracks across the North Atlantic (Stenseth *et al.*,2003). It is highly correlated with the Arctic oscillation, as it is

a part of it (see Fig.13 at Appendix B). The NAO was discovered in the 1920s by Sir Gilbert Walker. Unlike the El Niño phenomenon in the Pacific Ocean, the NAO is a largely atmospheric mode. It is one of the most important manifestations of climate fluctuations in the North Atlantic and surrounding humid climates. The North Atlantic Oscillation is closely related to the Arctic oscillation but should not be confused with the Oscillation Westerly winds blowing across the Atlantic, bring moist air into Europe. In years when westerlies are strong, summers are cool, winters are mild and rain is frequent. If westerlies are suppressed, the temperature is more extreme in summer and winter leading to heatwaves, deep freezes and reduced rainfall.The North Atlantic Current (North Atlantic Drift and the North Atlantic Sea Movement) is a powerful warm ocean current that continues the Gulf Stream northeast. West of Ireland it splits in two. One branch (the Canary Current) goes south while the other continues north along the coast of northwestern Europe where it has a considerable warming influence on the climate. Other branches include the Irminger Current and the Norwegian Current. Driven by the global thermohaline circulation (THC), the North Atlantic Current is also often considered part of the wind-driven Gulf Stream which goes further east and north from the North American coast, across the Atlantic and into the Arctic Ocean.

The variations in seasonal rainfall in Southern Europe during the present century, has relationships with the North Atlantic Oscillation (NAO) and the El Niño-Southern Oscillation (Stenseth *et al.*, 2003).

4.2 Northern Atlantic Oscillation Index (NAOI)

It is known from observations that the North Atlantic Oscillation(NAO) is the dominant, large-scale, extra-tropical teleconnection pattern in the Atlantic sector (Bjerknes,1964; Hurrell and Van Loon, 1997). Its phase is indicated by the NAO index (NAOI), which

measures the pressure difference between Portugal and Iceland. It is therefore related to the strength and position of maximum surface westerlies across the Atlantic and into Europe (Van Loon and Rogers, 1978). During the positive NAO phase relatively warm and moist air masses are advected by stronger than usual winter storms into northern Europe (Visbeck *et al*., 1998). Fig 14 shows the NAO Index calculated from 1860 to 2000 with intervals of 20years and Fig 5 at Appendix B, shows NAO Index from 1900 to 2000.

5. Upwelling

Upwelling is a phenomenon that occurs in a number of places in the global ocean. The term refers to cold, nutrient rich water coming to the surface from depths of over 50 meters. It is created by wind blowing across the ocean surface and pulling the surface water with it. As the surface water leaves an area, the 'hole' left behind is filled in by water 'upwelling' from below. Upwellings are important because they move cold and rich nutrient-rich water to the surface, provide nutrients to the photic zone and increase primary productivity.(NOAA, 2009 (http://oceanexplorer.noaa.gov/explorations)).

People in Peru have come to rely on cool, deep water to rise and bring nutrients to the surface. The small fish that are their livelihood eat the microscopic marine plants that use these nutrients. There are years where the cool, nutrient rich water comes to the surface, supporting enough fish for everyone. Some years there are hardly any fish. These years are tough on the coastal people who make their living from fishing. Can the fluctuations be predicted? Is Peru the only place where there are such a fluctuations? (NOAA, 2009 (http://oceanexplorer.noaa.gov/explorations)), see also Fig. 16 at Appendix B. Upwelling areas can be highly variable. There are climatologically events, such as El Nino, that reduce upwelling significantly. During El Nino events, the wind patterns change and thus the upwelling patterns change.

5.1. Downwelling

This is the downward current of surface water in the ocean, and is usually caused by differences in the density of seawater.. In the ocean, it often refers to where Ekman transport causes surface waters to converge or impinge on the coast, displacing surface waters to converge or impinge on the coast, displacing surface water downward thickening the surface layer. See Fig.17b at Appendix B. The net downwelling is determined by the geostrophic flow toward the boundary and is carried downward in a very narrow boundary layer of width E-1/3, where E is the Ekman number. For the calculations here, this boundary layer is O(100 m) wide. (Ings *et al.*, 2008). The model simulations show a high degree of skill for all variables evaluated with the Automatic Weather Station (AWS) data (pressure, temperature, water vapor mixing ratio, wind speed and direction, downwelling shortwave radiation, and net radiation) for all seasons, although the use of a fixed albedo in the Polar MM5 leads to large errors in the simulated net radiation budget over melting ice surfaces during the summer months. The modeled precipitation distribution agrees with available observations in the interior of the ice sheet but is excessive along the steep margins of the island. A discussion of possible future applications of the Polar MM5 is presented (Bromwich *et al.*, 2004).

5.2. Mechanisms that Cause Ocean Upwelling

There are two things that may cause Upwelling and these are;1)Water masses moving apart 2)Water moving away from land see Fig. 17,18 A and B at Appendix B respectively. Other mechanisms that create upwelling are: Wind, Coriolis Effect and Ekman Transport. In order to understand the different types of upwelling, the Coriolis Effect and Ekman Transport need to be introduced. The Coriolis Effect is the apparent

curvature of the path of a moving object due to the fact that Earth rotates underneath it as it moves. The water in the ocean moves in accordance with this Coriolis Effect as well. It is not 'attached' to the Earth and so moves in an apparently curved path. The curvature is to the right of movement in the Northern Hemisphere, and to the left of the movement in the Southern (NOAA, 2009), sees fig19A and 19B at Appendix B.

5.2.1. Physical application of Upwelling

Upwelling has significant influence on the Physical processes in that subsurface water rises towards the surface and since the temperature of the water generally with decreases with depth, upwelled water is colder than the surface water it replaces.Therefore,in an upwelling area, surface temperature is usually colder than surrounding temperatures.Fig.20 and 21 at Appendix B show the process of water brought to the surface and colder temperature along the coastline shown in dark blue respectively (Conway, 1997).

The Sagres area is subjected to the upwelling of cold waters in spring to late summer, originating in the wind-driven circulation patterns off the south and west coast (Loureiro *et al*, 2005).

5.3. The Coriolis Effect

Oceanographers have long sought to verify the theoretical Ekman transport relation, which predicts that a steady wind stress acting together with the Coriolis force will produce a transport of water to the right of the wind(Price *et al.*, 1987). By averaging all the movement of the water from the surface to the Ekman Depth, Ekman Transport is derived. Ekman Transport is the net effect of the wind on all these frictionally bound surface layers and is 90^{o} to the wind. For example, with a northward blowing wind in

the northern hemisphere, Ekman Transport will be to the right of the path or eastward. See Fig.22A and 22B at Appendix B.

5.3.1. Climatic rainfall

Upwelling is capable of influencing meteorological conditions such as rainfall in the region surrounding the upwelling area. The colder water associated with upwelling can significantly inhibit thunderstorm development. If this upwelled water is cooler than the air, it can cool the air sufficiently to form fog and low clouds called stratus. This will create areas of unequal surface heating which leads to development of surface fronts in the atmosphere along the boundary between upwelled and non-upwelled water, or between upwelled water and adjacent land (Conway, 1997). Fig.23 at Appendix B showing annual rainfall of the world and this can be related to areas of upwelling Fig.1 and 2 at Appendix B.

Coastal upwelling can have a negative effect on inland rainfall in that as wind blows across the coastline, and meets warmer air from the land, water vapour near the coast condenses and this results in rainfall over the ocean leaving the land dry. Examples of these are as follows:

- Mauritania –the Sahara Desert (Fig.23a at Appendix B)
- Namibia-Kalahari Desert (Fig.23b at Appendix B)
- Peru- Atacama Desert

Cold upwelled waters off the western coast of Africa generally prevent tropical disturbances from forming into stronger tropical storms and hurricanes that could eventually affect North America.(Conway, 1997).

5.4. Types of Upwelling

There are three main types of upwelling; coastal, equatorial and seasonal.

5.4.1. Coastal upwelling

Rather than being in the open ocean, coastal upwelling occurs along the border of a continent. For example, the main wind-driven current along the west coast of the United States is southward (the California Current). As the water moves southward, Ekman Transport is to the right of the path (westward), or away from the coast. As the coastal area has a deficit of water, upwelling will occur. Coastal upwelling is most prominent along the California and Oregon coasts, the Peru coast, the south-western tip of Africa and the north-western tip of Africa. Fig24. at Appendix B illustrates this type of upwelling.

5.4.2. Equatorial upwelling

This is caused by the winds known as the trade winds. The trade winds blow from east to west in the vicinity of the equator. On the northern side of the equator Ekman Transport is to the right (northward), and on the southern side it is to the left (southward). With water flowing directly away from the equator, both northward and southward, the equator itself has a deficit of water. Hence, water from below upwells to fill in the gap. Equatorial upwelling is most prominent in the Pacific Ocean. See Fig.25 at Appendix B.

5.4.3. Seasonal upwelling

This occurs due to 180^{o} shifts in the direction of wind due to land/water heating differences between summer and winter. In the summer, land heats a great deal compared to water and the heated air over land rises, thus inviting wind to blow toward land from water (onshore). In the winter, land cools more significantly than water so the relatively warm air over water rises, thus inviting wind to blow toward water from land

(offshore). In the first case, there will be a pile up of water at the coastline. In the second case, there will be a removal of water from the coastline. This will be an invitation for upwelling along the coast. See Fig.26 at Appendix B.

5.5. Sea Surface Temperatures (SSTs)

Warming is larger in the Western Equatorial Pacific than in the Eastern Equatorial Pacific over the past century, and it was suggested that the increased West–East temperature gradient may have increased the likelihood of strong El Niños, such as those of 1983 and 1998. Comparison of measured sea surface temperatures in the Western Pacific with pale climate data suggests that this critical ocean region, and probably the planet as a whole, is approximately as warm now as at the Holocene maximum and within 1°C of the maximum temperature of the past million years (Hansen *et al.*, 2006).

The satellite measured SST provides both a synoptic view of the ocean and a high frequency of repeat views, allowing the examination of basin-wide upper ocean dynamics not possible with ships or buoys. For example, a ship traveling at 10 knots (20 km/h) would require 10 years to cover the same area a satellite covers in two minutes. The Group for High resolution SST (Donlon *et al.*, 2007),provides operational access to nearly all satellite SST data sets in a common format and within 6 hours of acquisition by the satellite instrument. Fig. 27 at Appendix B is showing the global sea surface temperature and ice analysis SST indicates a generally warming across the tropics as well as the mid latitudes. SST's are also used in seasonal forecast of either temperature or rainfall. For example, Indian monsoon rainfall in most uncoupled models is positively correlated to tropical Indian Ocean SST's because of higher moisture fluxes (Mason, 2008).

5.5.1 Identifying Upwelling on Satellite-derived Maps

One method of identifying areas of upwelling is to look at Sea Surface Temperature (SST). Because the water that is upwelled is very cold, we can look at satellite-derived temperature maps of the water surface to find areas that show colder temperatures than surrounding water. The surrounding water will be warmer as the sun has warmed it for a longer period of time. Due to the way the earth is tilted and rotates around the sun, the sun warms the earth more in latitudes near the equator and less toward the poles. Therefore, areas of upwelling will stand out as 'too cold' for a given latitude. See Fig.28 at Appendix B. An example is forecasting coastal upwellings in Lake Michigan using satellite derived temperature images and buoy data (Plattner *et al.*, 2006).

5.6. Remote sensing

Another way to identify areas of upwelling is by using maps of Ocean Color. These are maps of chlorophyll on the surface of the ocean. Chlorophyll is a telling signal of upwelling due to the fact that upwelled water brings with it nutrients and dissolved gases that are important for plant growth. The list includes nitrogen, phosphorous, silica and carbon dioxide. With these being brought to the surface, where sunlight is also available, marine plants including microscopic phytoplankton (algae) grow very well. Hence, the chlorophyll that they contain can be used to identify areas where upwelling is occurring. In remote sensing energy emanating from the earth's surface is measured using a sensor mounted on an aircraft or spacecraft platform. That measurement is used to construct an image of the landscape beneath the platform, as depicted in Fig.29 at Appendix B (Richards and Jia, 2006). Fig 30.is showing ocean color map of the world.

5.7.Biological effect on upwelling

The total primary production in the water column depends not only on the intensity of light at the surface but how far down they penetrate. If the photic zone is deep there will be lots of primary production. The depth of the photic zone varies with season and is deepest in summer. On cloudy days, the photic zone is not as deep as on a clear day. In dirty water (sediments, oil, pollution) light does not penetrate as deep. The phytoplankton themselves absorb light for photosynthesis thus they cut down the amount of light for deeper dwelling phytoplankton. This phenomenon is called self-shading. The deeper dwelling phytoplankton can absorb light of deeper penetrating wave lengths. Self-shading is important in highly productive murky waters because they contain so much plankton. Conversely, the barren waters of the central gyres in the middle of ocean basins are incredibly clear (Bricaud *et al.*, 1995). Primary production is a fundamental biological process in the ocean carbon cycle. Because primary production is driven by photons from solar radiation, the absorption of light by phytoplankton cells is one of the essential links in a description of primary production and phytoplankton growth .Phytoplankton absorption is also one of the most important factors to control the irradiation field of the open ocean.(Harimoto *et al.*, 1999).Fig.31 at Appendix B.is indicating the marine ecosystem.

The surface area of the coastal zone is about 7% of the total surface area of the ocean ; Total annual primary production in the coastal zone has been estimated to be ~20% of total ocean production (Wollast, 1998). The primary production of the world is shown in Fig.32 at Appendix B.

5.8. Chlorophyll

Phytoplanktons are microscopic floating plants that contain chlorophyll and hence obtain energy for growth by photosynthesis. These tiny organisms perform nearly all the

photosynthesis in the Open Ocean (Bricaud *et al*., 1995). See Fig.33, at Appendix B , which is showing chlorophyll concentrations. Phytoplanktons photosynthesize using specialized color pigments called chlorophyll. Thus, "Ocean Color" maps are another way to identify areas of upwelling, as in Fig.30 at Appendix B. The factors doing effect on vertical distribution of Chlorophyll are the environmental conditions which are: Light, Nutrients and Temperature.

The vertical distribution of Chl-*a* in mixed layer depends on mixing intensity relative to a rate of phytoplankton acclimation to light. The correlation is there between surface chlorophyll and depth of euphotic zone is negative. The downwelling *irradiance* (Ed) diminishes in an exponential manner with depth (z):

$Ed(z)=Ed_0 \exp(-kz)$, (kz) – optical depth (ς). $\varsigma(kz)=\ln (Ed(0)/ Ed(z)$

$\varsigma(1\%)=\ln(100/1)=\ln(10)\times \lg(100)$ $\varsigma(1\%)=2.3\times2=4.6$

$Z_{eu}=4.6/k$ $Z_{eu}=3.19\ Z_{sd}$, (Kirk, 1983)

$Z_{eu}=2.7\text{-}3.0\ Z_{sd}$ (For the Black Sea) Z_{sd} – represents the Secchi depth

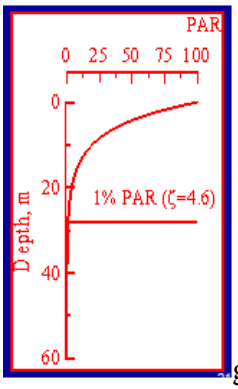

graph showing the irradiance(light) with depth. (Fujika *et al.*, 2002).

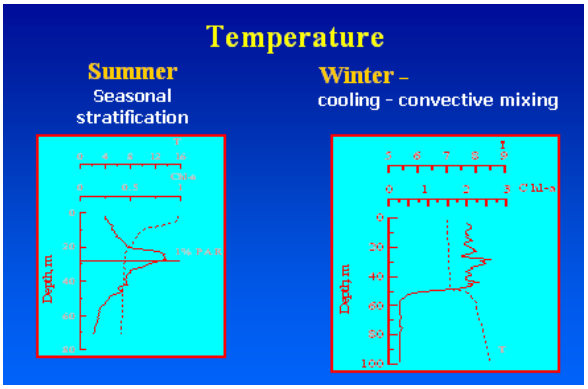

Two quasi-isolated layers in the diagram above are appeared due to seasonal water stratification. This is the temperature effect on the vertical distribution of Chlorophyll. The graphs below show the nutrients effect on the vertical distribution of Chlorophyll.

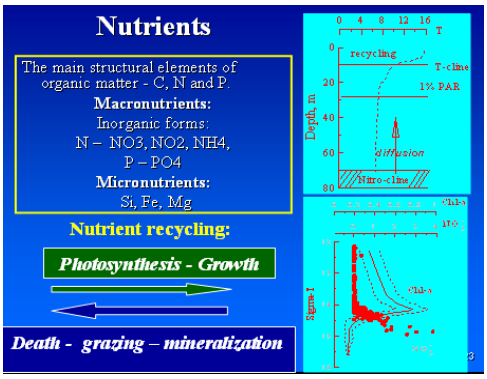

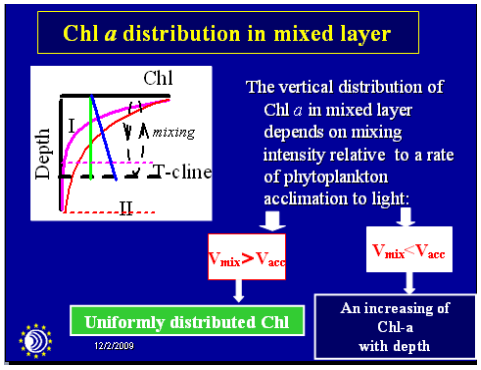

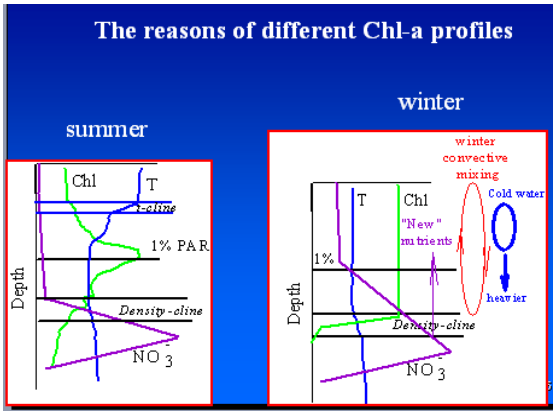

Chl-a profiles (for stratified waters:

Gaussian formulation according to Platt et al. (1991)

$$C_a(z) = C_0 + (h/\sigma\sqrt{2\pi}) * \exp[-(z - z_m)^2 / 2\sigma^2]$$

h of the maximum;

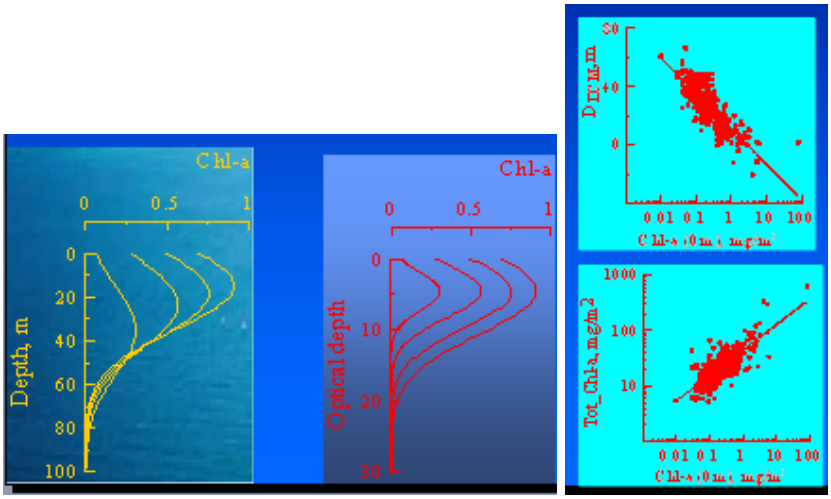

Pigment-Phytoplankton biomass ratio

Chlorophyll concentration in water**;**

mgChl/m3 =

N cell/m3 × Chl/cell

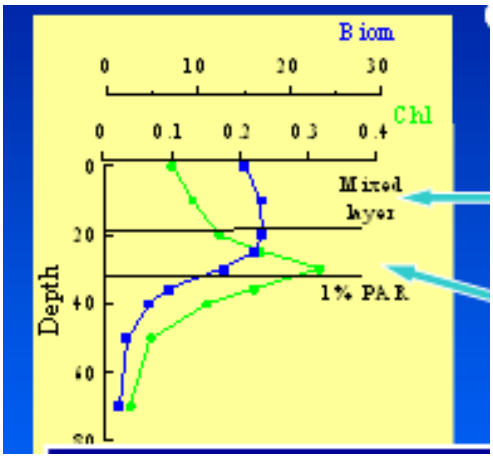

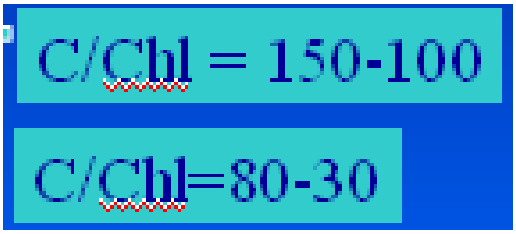

The Chl-a profile does not reflect phytoplankton biomass profile, because intracellular pigment concentration changes with depth resulting from acclimation to environmental factors (Bricaud *et al*, 1995).

Intracellular pigment content:

Chl/C ratio increases when irradiance and nutrient limitation decreases;

Temperature increases: see graph below:

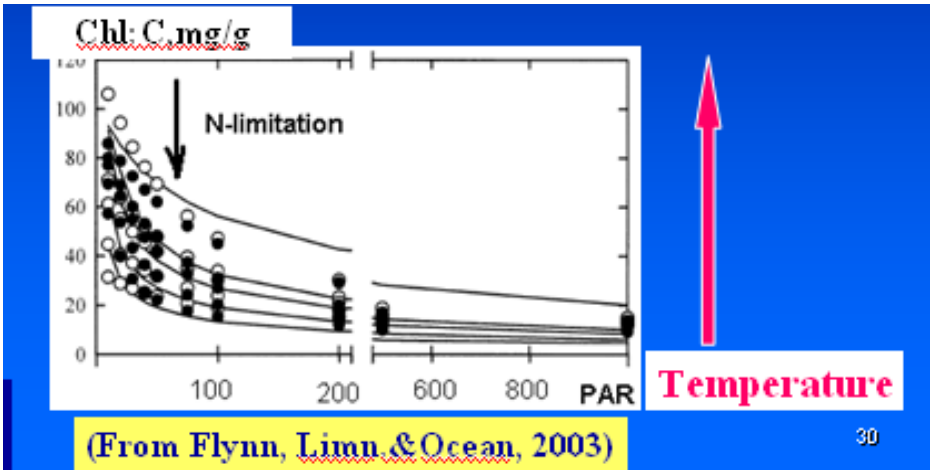

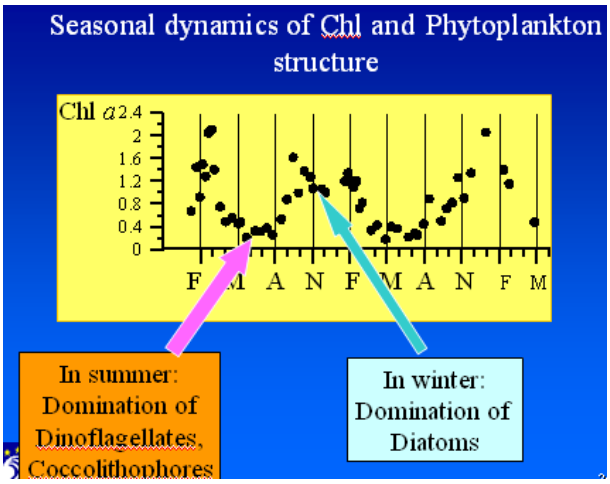

The reasons of variability in Chl and Phytoplankton profiles in shelf waters are:
Storm, horizontal advection, eddy and upwelling

In upwelling areas the "new" nutrients come into upper layer resulting in an increasing

of primary productivity ("new" production) the graphs indicates (Fujika *et al.*, 2002).

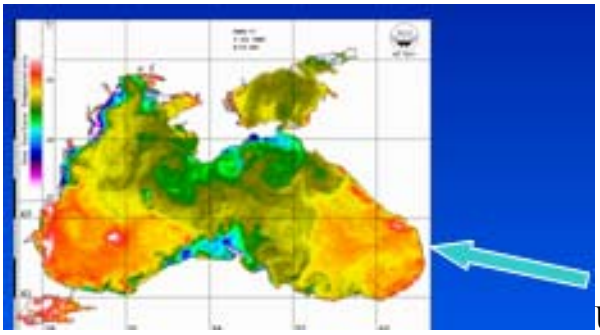
Upwelling

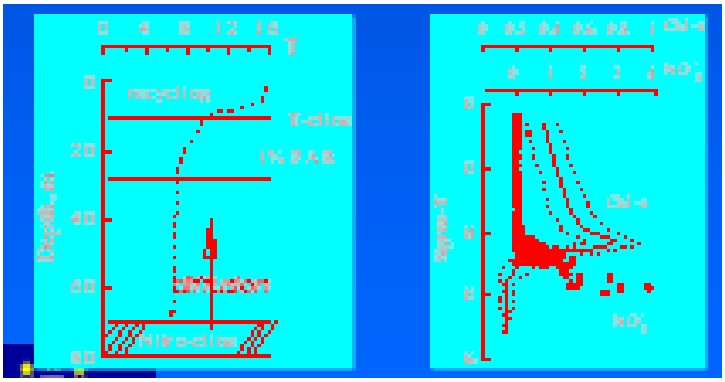

It was shown that the spatial relationship between SST, [Chl] and the advective patterns is not fixed during course of the upwelling event. When the intensity of the northerly wind component was higher than 5 m/s, there is an asymmetry between the [Chl] and surface temperature distributions, with low [Chl] values along the cold filament axis and higher [Chl] values along the southern filament boundaries.(Oliveira *et al.*, 2009).

6. References

Bjerknes, J. (1964). Atlantic air-sea interaction. Adv. Geophys., Vol.10: 1-82.

Bricaud. A, Babin M.Morel A, Claustre H, (1995), Variability in the Chlorophyll-Specific absorption coefficients of natural phytoplankton: Analysis and parameterization, Journal of Geophysical Research. Vol. 100. N0.7.p.13321-13332.

Bromwich, D. H; Toracinta,E.R.,Wei,H.,Oglesby,R.J.;Fastook,J.L.,Hughes,T.J.(2004). Polar MM5 simulations of the winter climate of the Laurentide Ice Sheet at the LGM, American Meteorological Society. 17**:** 3415-3433.

Conway, E. D. (1997). An introduction to satellite image interpretation, Johns Hopkins Univ Pr. Maryland Space Grant Consortium, The Johns Hopkins University Press, Baltimore, 242 p. ISBN 0 8018 5576 4.

Diehl JM, Toonen RJ, Botsford L.W,(2007) Spatial variability of recruitment in the sand crab Emerita analoga throughout California in relation to wind-driven currents. Mar Ecol Prog Ser 350:1–17.

Donlon,C.,Robinson,I.,Casey,K.,Vasquez,J.,Armstrong,E.,Gentemann,C.,May,D.,LeBorgne,P,Pioll,J,Barton,I.2007). The Global Ocean Data Assimilation Project (GODAE) High Resolution Sea Surface Temperature Pilot Project (GHRSST-. 88: 1197-1213. PP).

Ellison, J. C.(2009). Wetlands of the Pacific Island region, Wetlands Ecology and Management, 17 (3). pp. 169-206. ISSN 0923-4861. Newland, C and Field, IC and Nichols Springer. 1**7:** 169-206.

Entekhabi, D.(1990). Land surface hydrology parameterization for atmospheric general circulation models: subgrid spatial variability and sensitivities in a simple climate model, Journal of climate. Volume 2. 816-831, Massachusetts Institute of Technology.

Fujika T., S.Taguchi. (2002), Variability in chlorophylla specific absorption coefficient in marine Phytoplankton as a function of cell size and irradiance. Plankton Research V.24. N0.9. p.859-874.

Hansen, J.,Sato,M.,Ruedy,R.,Lo,K.,Lea,D.W.,Medina-Elizade,M. (2006). Global temperature change, National Acad Sciences. PNAS 103**:** 14288.

Harimoto, T., Ishizaka,J.,Tsuda,R.(1999).Latitudinal and vertical distributions of phytoplankton absorption spectra in the central North Pacific during spring 1994, J. Oceanography**. 55:** 667-679.

Hurrell, J. W., Kushnir,Y.,Ottersen,G.,Visbeck,M.(2003).An overview of the North Atlantic oscillation,Aagu American Geophysical Union. 134: 1-36.

Hurrell, J. W. and H. Van Loon (1997). Decadal variations in climate associated with the North Atlantic Oscillation, Climate Change 36:301 326 **.** climate events and public health responses. Dresden,Springer.

Ings, D. W., Gregory, R.S.,Schneider, D.C.(2008).Episodic downwelling predicts recruitment of Atlantic cod, Greenland cod and white hake to Newfoundland coastal waters, Sears Foundation for Marine Research. 66: 529-561.

Kushnir, Y. (1994). Interdecadal variations in North Atlantic sea surface temperature and associated atmospheric conditions, Boston, MA: American Meteorological Society, c1988-. **7:** 141-157.

Loureiro, S.,Newton,A,Icely,J.D.(2005). Microplankton composition, production and upwelling dynamics in Sagres (SW Portugal) during summer of 2001. Scientia Marina,69. 323-341.

Mason, S. J. (2008).From Dynamical Model Predictions to Seasonal Climate Forecasts, NATO Science Series, Academic Publishers, 205-234Springer.

Oliveira, P. B., Nolasco,R., Dubert,J.,Moita,T.,Peliz.(2009). Surface temperature, chlorophyll and advection patterns during a summer upwelling event off central Portugal, Continental Shelf Research, Volume 29, Issues 5-6, 30 March 2009, Pages 759-774.

Peliz, Rosa, T. L.,Santos, A.M.P., Pissarra, J.L. (2002). Fronts, jets, and counter- flows in the Western Iberian upwelling system,Jounal of Marine System 35: 61-77.

Picaut,J.,Ioualalen,M.,Menkes,C.,Delcroix,T.,McPhaden,M.J.(1996). Mechanism of the zonal displacements of the Pacific warm pool: Implications for ENSO, Science 274: 1486-1489,AAAS. 274**:** 1486.

Plattner,S.,Mason,D.M.,Leshkevich,G.A,Schwab,D.J.,Rutherford,E.S.(2006). Classifying and forecasting coastal upwellings in Lake Michigan using satellite derived temperature images and buoy data, BioOne. 32**:** 63-76.

Prange, M.and M.Schulz. (2004). A coastal upwelling seesaw in the Atlantic Ocean as a result of the closure of the Central American Seaway (CAS),Citeseer:31:17207-17209

Price, J. F.,Weller, R. A.,Schudlich,R.R. (1987). Wind-driven ocean currents and Ekman transport, AAAS. 238**:** 1534.

Relvas, P., Barton, E.D. (2002). Mesoscale patterns in the Cape São Vicente (Iberian Peninsula). J. Geophys. Res. 107, 3164, doi: 10.1029/2000JC000456.

Relvas, P. And Barton, E. D., (2005). A separated jet and coastal counterflow during upwelling relaxation off Cape Sao Vicente (Iberian Peninsula), The Guajira upwelling. Continental Shelf Research, 25, 29-49.

Richards, J. A. and X. Jia,(2006). Remote sensing digital image analysis: an introduction, Springer Verlag.

Schluessel, P., Emery, W. J., Grassl, H.,Mammen, T.(1990). On the bulk-skin temperature difference and its impact on satellite remote sensing of sea surface temperature, American Geophysical Union. 95.

Stenseth, N. C.; Ottersen,G.,Hurrell,J.W.,Mysterud,A.,Lima,M.,Chan,K.S.,Yoccoz, N.G.,Adlandsvik,B.(2003). Studying climate effects on ecology through the use of climate indices: the North Atlantic Oscillation, El Nino Southern Oscillation and beyond. Proceedings of the Royal. Society of London, Series B. 270**:** 2087-2096.

Strass, V. H., (1992).Chlorophyll patchiness caused by mesoscale upwelling at fronts, Deep Sea Res., Part A, 39, 75–96.

Trenberth, K. E. 1997. The definition of El Nino, American Meteorological Society. 78: 2771-2777.

Van, L. H. y ROGERS, JC .1978.The Seesaw in Winter Temperatures between Greenland and Northern Europe. Part I: General Description? 106: 296-310.

Viboud, C.,Pakdaman, K., Flahault, A.; Boelle, P.Y.; Wilson, M. Myers, M.L.;Valleron, A.J.2004. Association of influenza epidemics with global climate variability, Impact of climate change 19**:** 1055-1059.

Visbeck, M.,Cullen, H.;Krahmann,G.,Naik,N.1998. Ocean model's response to North Atlantic Oscillation-like wind forcing. Geophysical Research Letters, 25: 4521-4524.

Wollast, R. 1998. Evaluation and comparison of the global carbon cycle in the coastal zone and in the open ocean. Estuarine Coastal and Shelf Science 10: 213?52.

Appendix B. Figures for Review

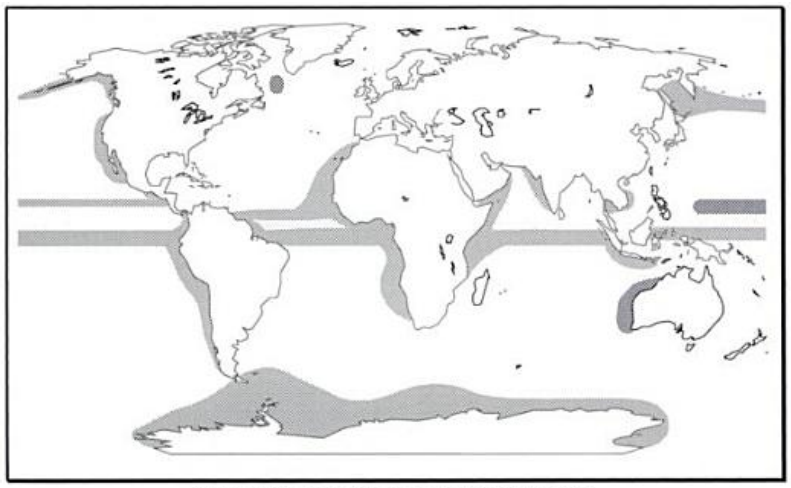

Fig.1. Showing General Areas of upwelling (Source: An Introduction to satellite image interpretation-By Prof. Eric.D.Conway, 1997).

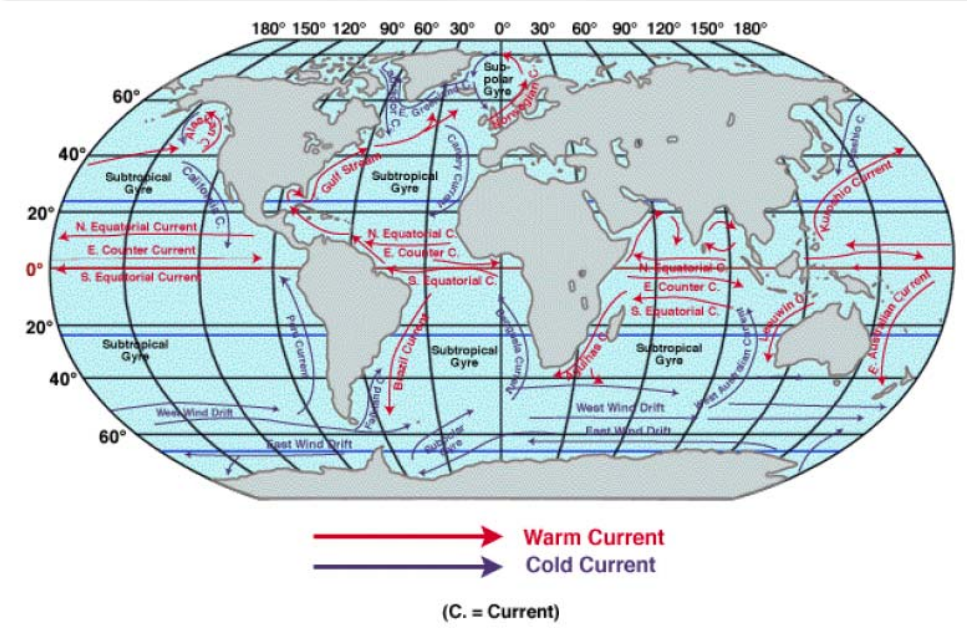

Fig.2. Showing warm and cold water current.(Source: Virtual Vacationland: Ocean Temperature)

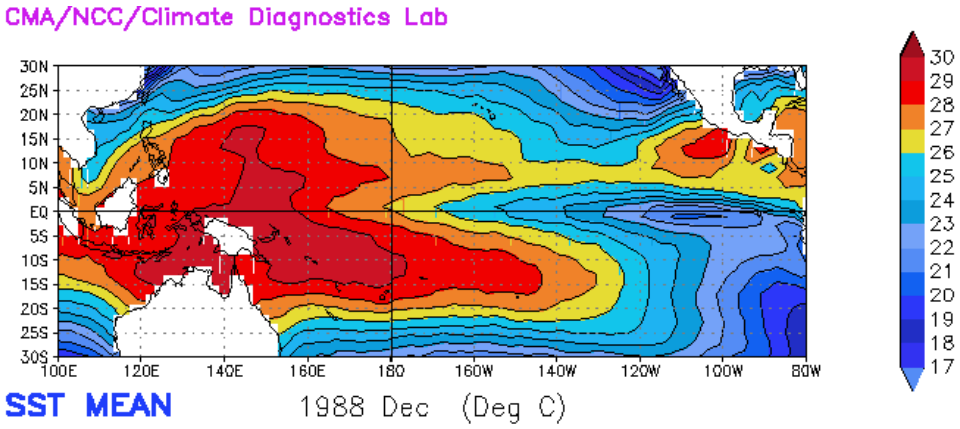

Fig3. El Nino-Southern Oscillation event (Source: National Climate Center, Beijing 1998/2000)

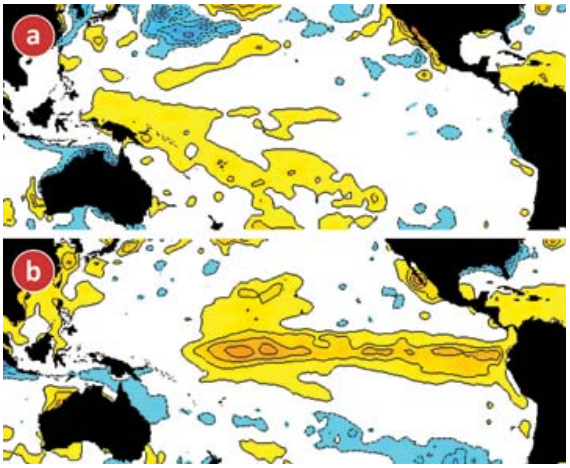

Fig.4. ENSO-Neutral conditions (a) compared to the warmer waters of a typical El Nino.
(b) Shown as sea surface temperature anomalies in the equatorial pacific ocean. From; IRI.

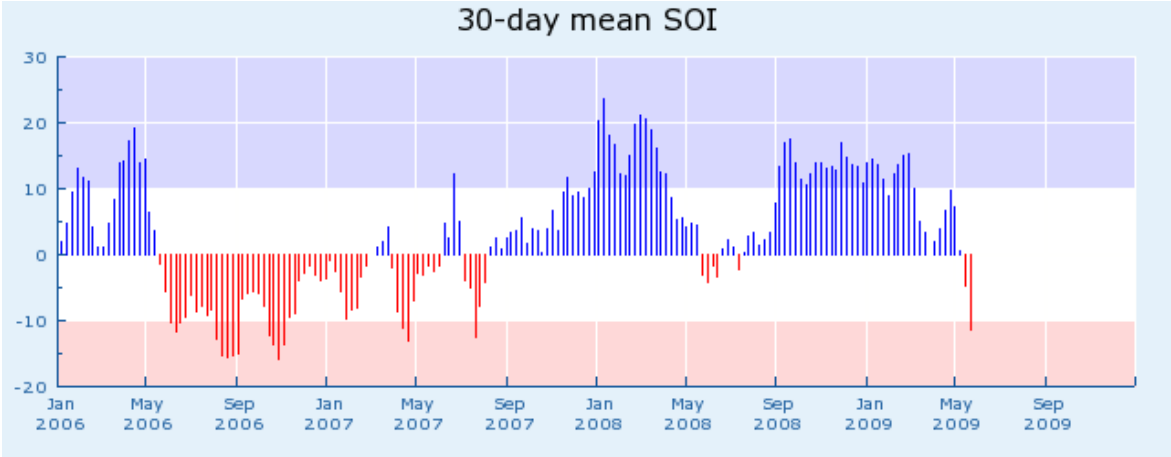

Fig.5. The Southern Oscillation Index (SOI) is calculated from the monthly or seasonal fluctuations in the air pressure difference between Tahiti and Darwin. Source: from http://en.wikipedia.org./wiki/EL-Nino

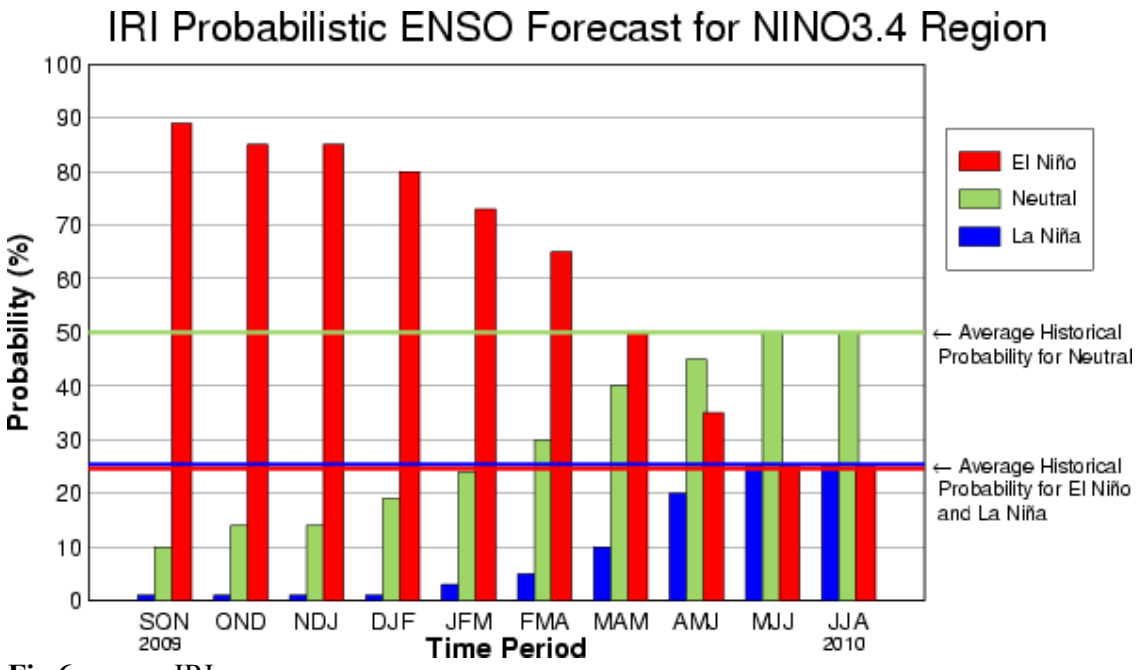

Fig.6. source:IRI

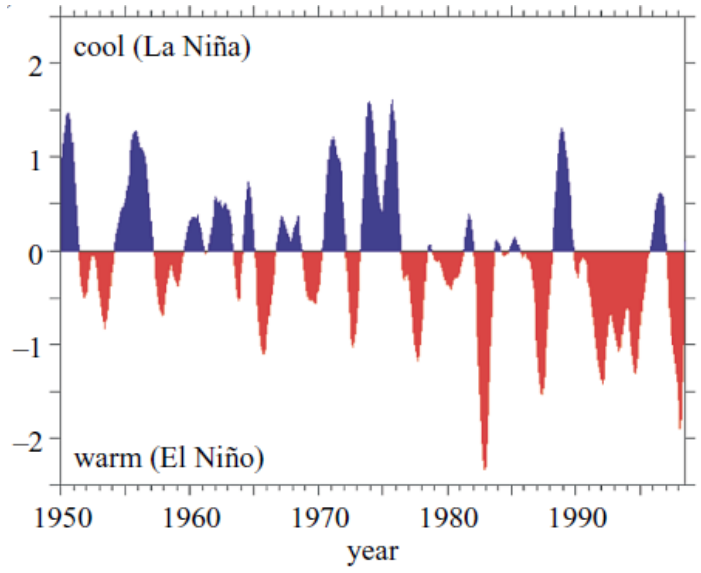

Fig.7. Normalized Tahiti minus Darwin SLP anomalies (from http://www.cgd.ucar.edu/cas/catalog/climind/soi.html) Source:(Stenseth, Ottersen et al. 2003)

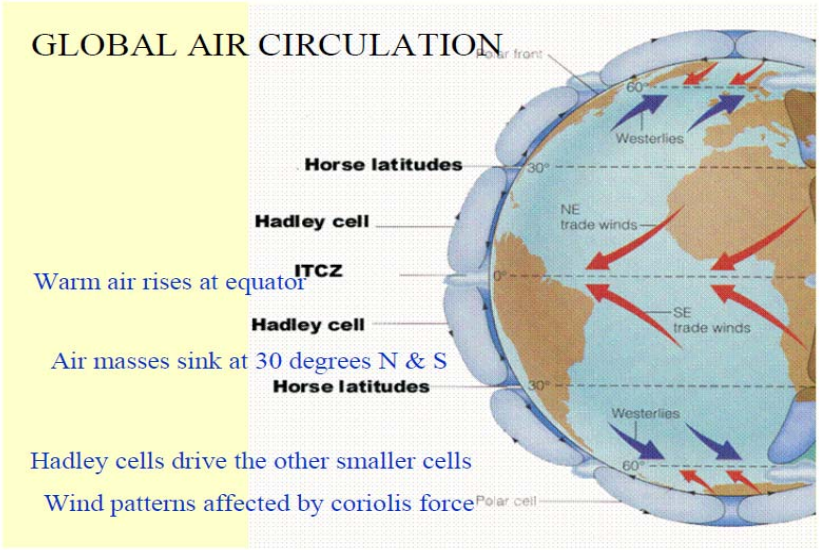

Fig.8. The general circulation

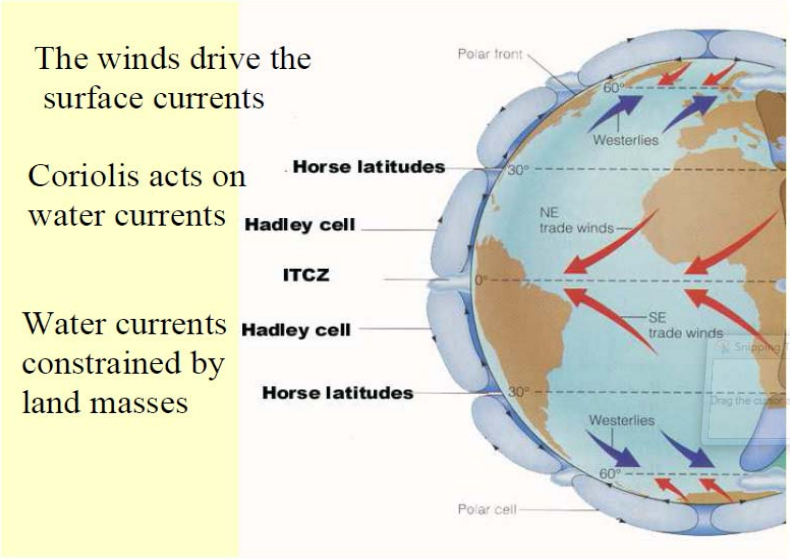

Fig 9 . Wind effect on surface water currents. Adapted from : NOAA / PMEL / TAO NOAA / PMEL / TAO.Key: for Fig.8&9
Red arrows = Trade winds
Blue arrows= Westerlies

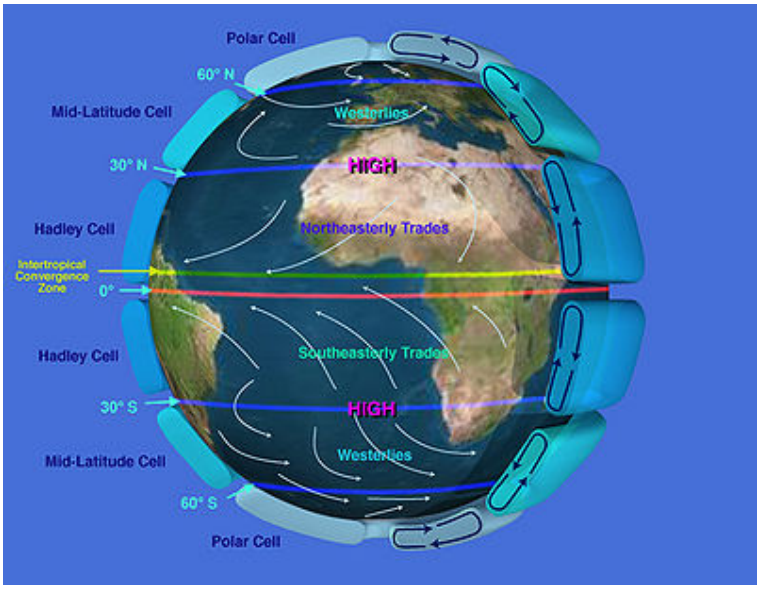

Fig.10. The trade winds are part of the Earth's atmospheric circulation From:http://en.wikipedia.org/wiki/Trade_wind

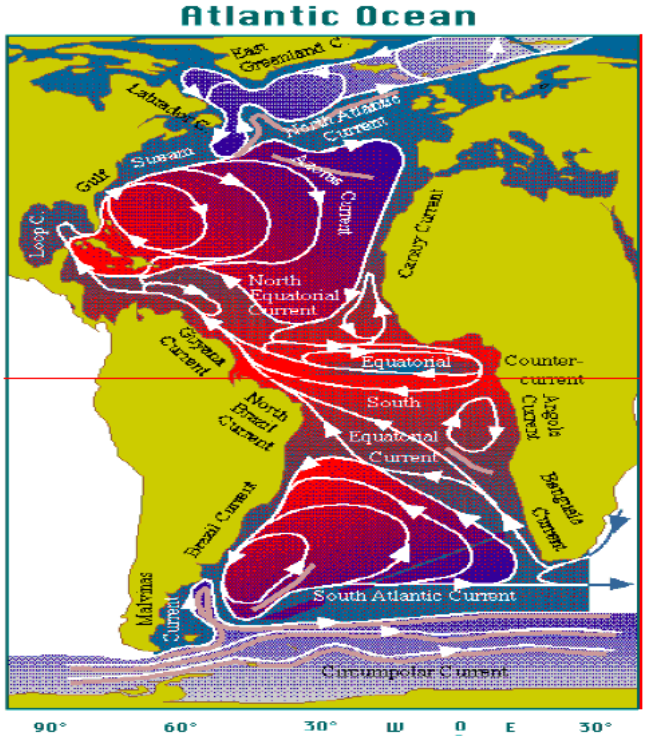

Fig.11. Atlantic Ocean circulation .(Source; Adapted from Barton 2001)

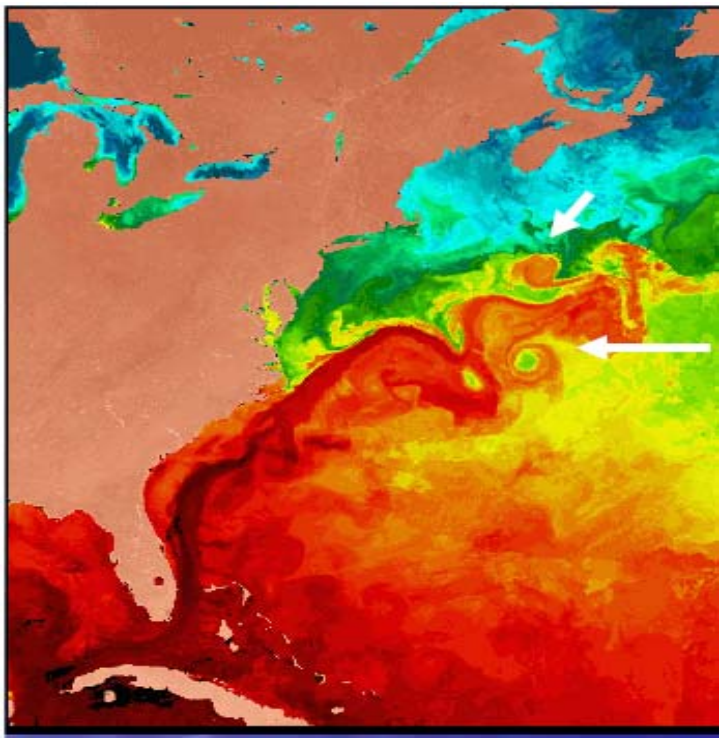

Fig12. This satellite sea-surface temperature image of the Gulf Stream illustrates the two types of eddies, or rings, as they are now called. (Source; (From oceansonline.com).

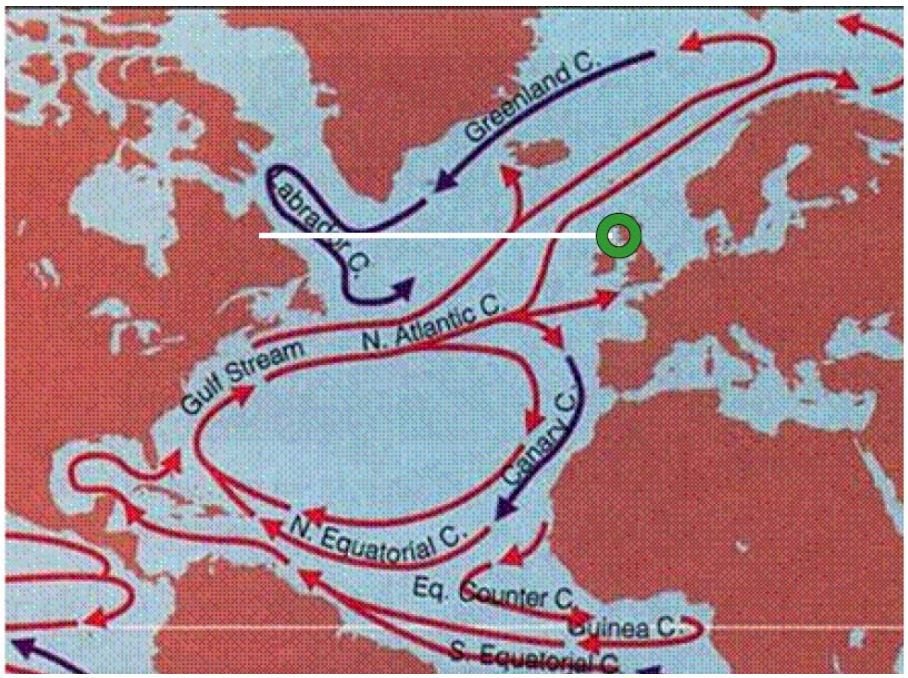

Fig.13. The general near surface circulation of the North Atlantic Ocean. (Source; Adapted from Barton 2001)

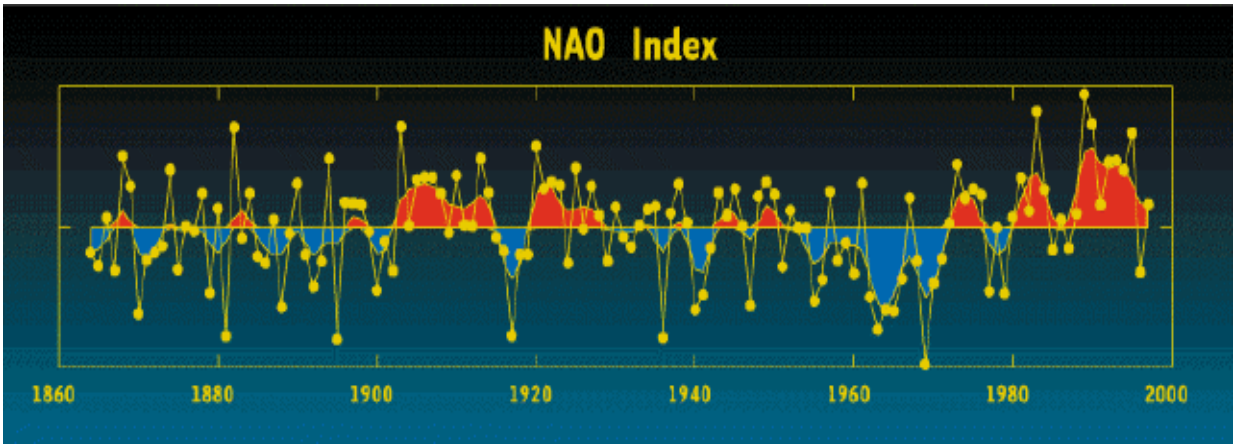

Fig.14. The NAO index is defined as the anomalous difference between the polar low and the subtropical high during the winter season (December through March) (source http://www.ldeo.columbia.edu/NAO by Martin Visb

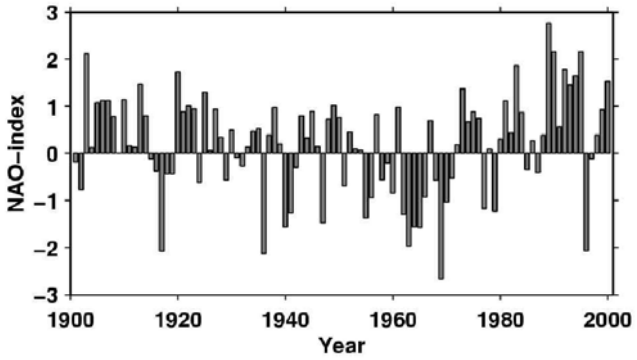

Fig.15. The North Atlantic Oscillation Index (source: Adapted from http://www.ldeo.columbia.edu/NAO by Martin Visbeck)

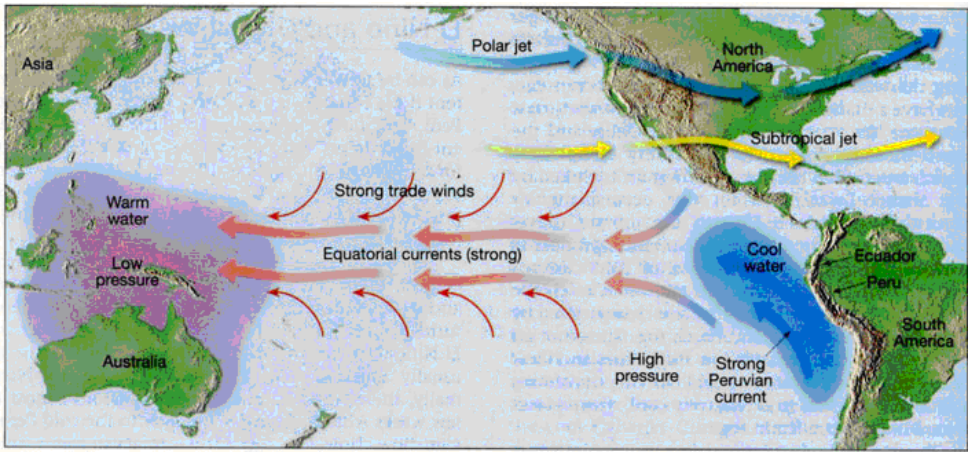

Fig.16. Source: Pierre Madl (2000)
Normally, the trade winds and strong equatorial currents flow toward the west. At the same time, an intense Peruvian current causes upwelling of cold water along the west coast of South America.

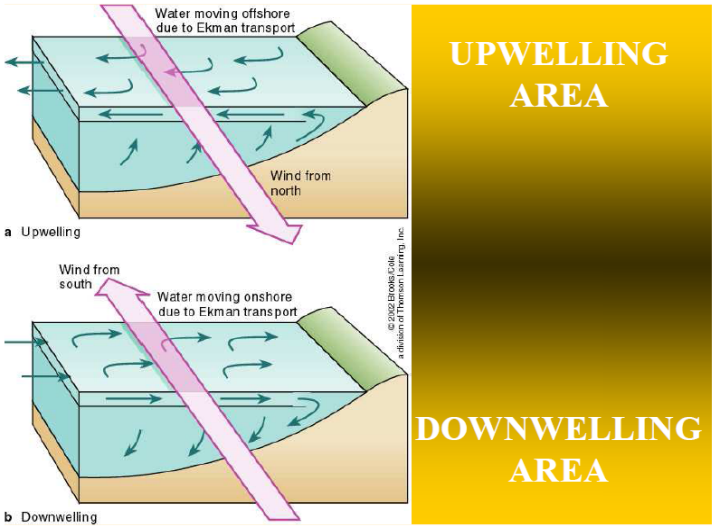

Fig.17.Showing Upwelling and Downwelling Areas

A 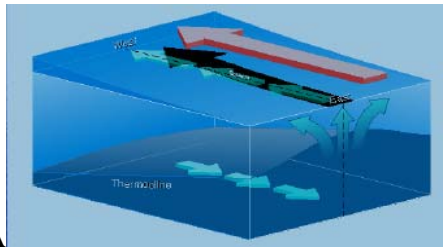

B 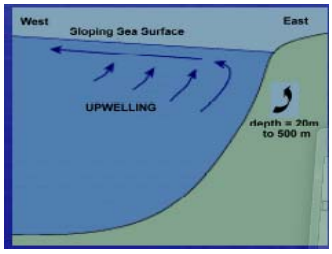

Fig.18. Causes of upwelling source: Adapted from Department of Atomspheric Sciences, Univesity of Illionois at Urbana Champaign

A 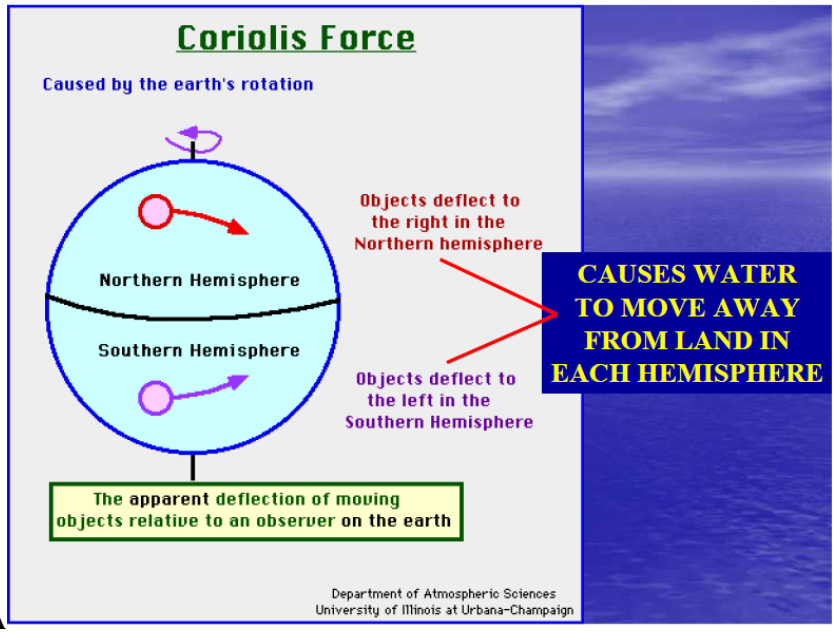

Fig19. A. The Coriolis force

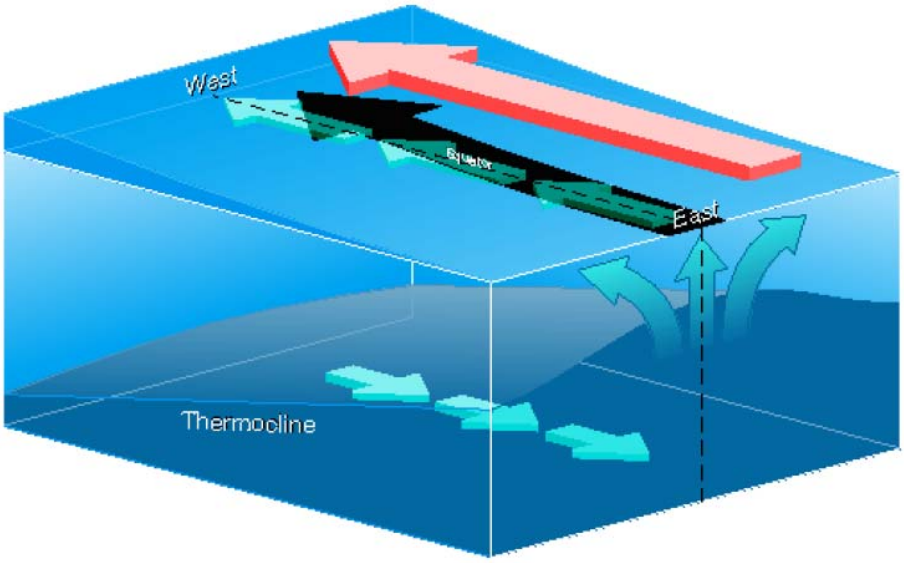

B The Coriolis Effect:Source:from: http://en.wikipedia.org/wiki/File:Upwelling.jpg

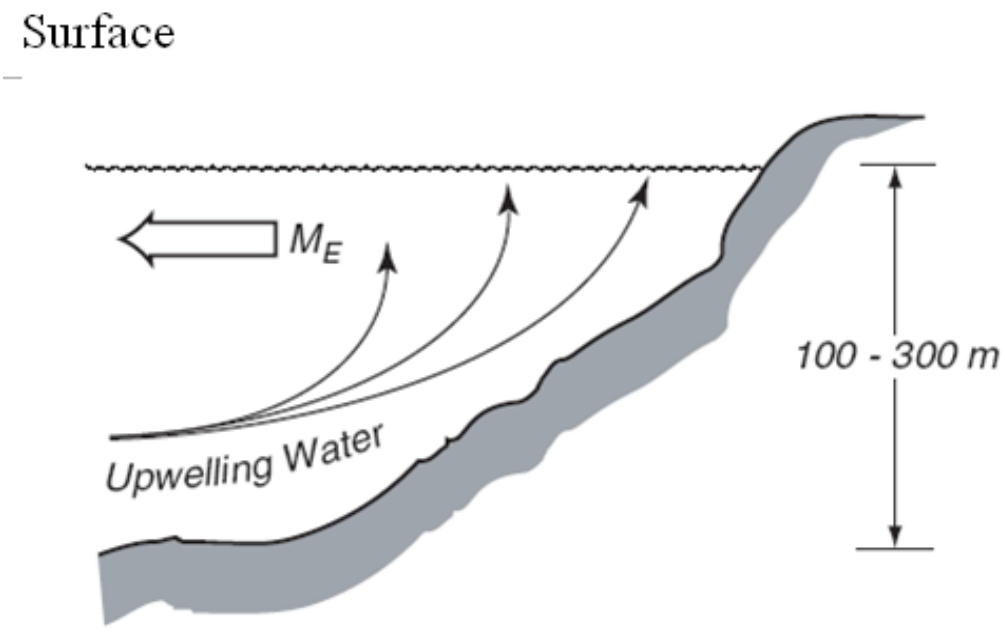

Fig.20. Cold water being upwelled to the surface.. Source Adupted from Microbiology procedure (http://www.microbiologyprocedure.com/microbial-ecology-of-different-ecosystems/marine-ecosystem-upwelling.html))

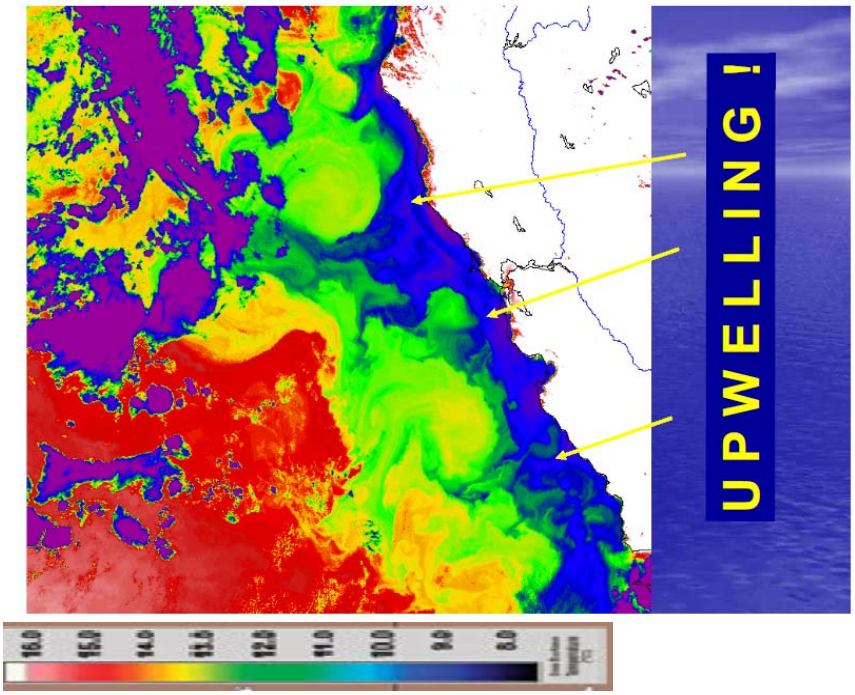

Fig.21. Sea surface temperatures during upwelling period. (Dark blue is coldest.) Image: NASA

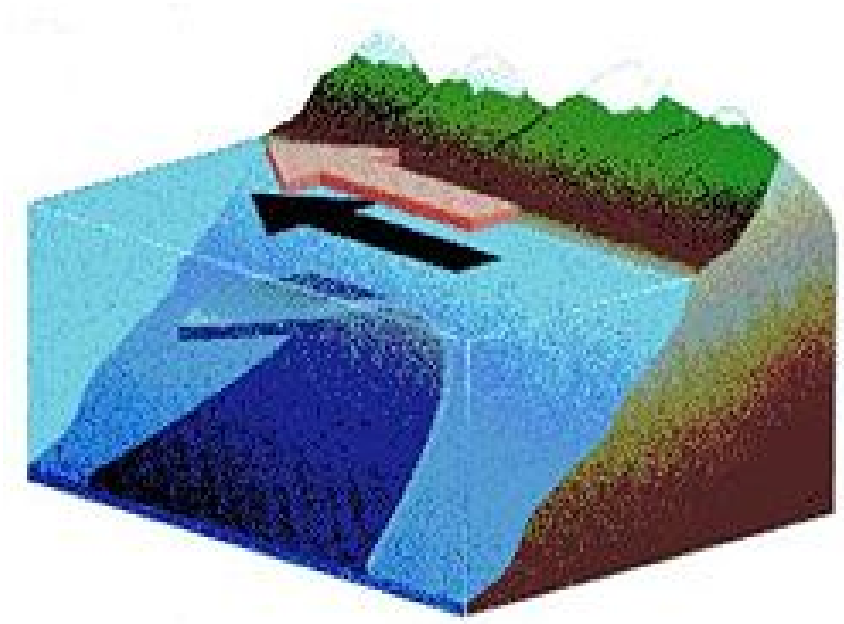

Fig.22.A. Upwelling near the coast due to Ekman transport perpendicular to the wind on the southern hemisphere.source; *adapted from: http://en.wikipedia.org/wiki/Ekman_transport*

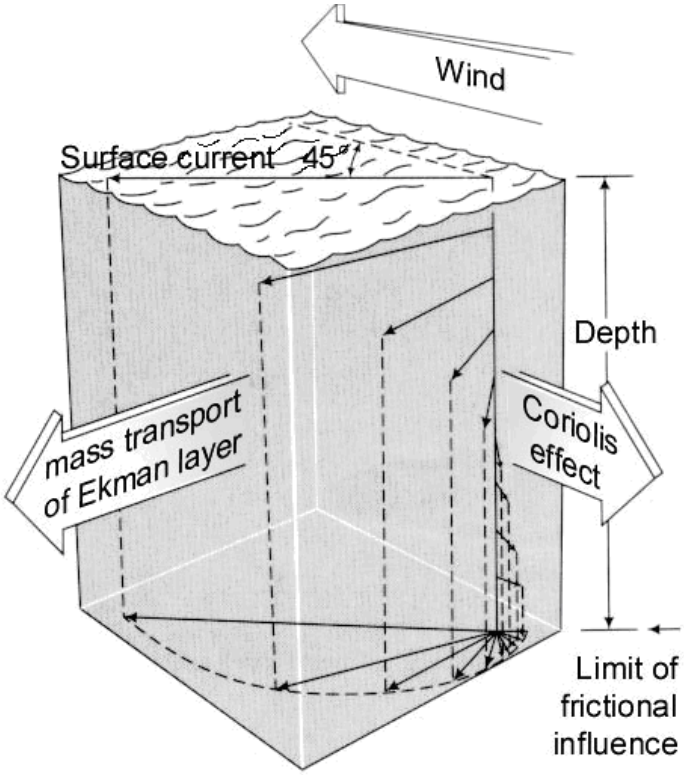

Fig.22B. The Ekman spiral (southern hemisphere) is believed to be the result of the action of steady wind on surface waters. Source: Pierre Madl (2000).

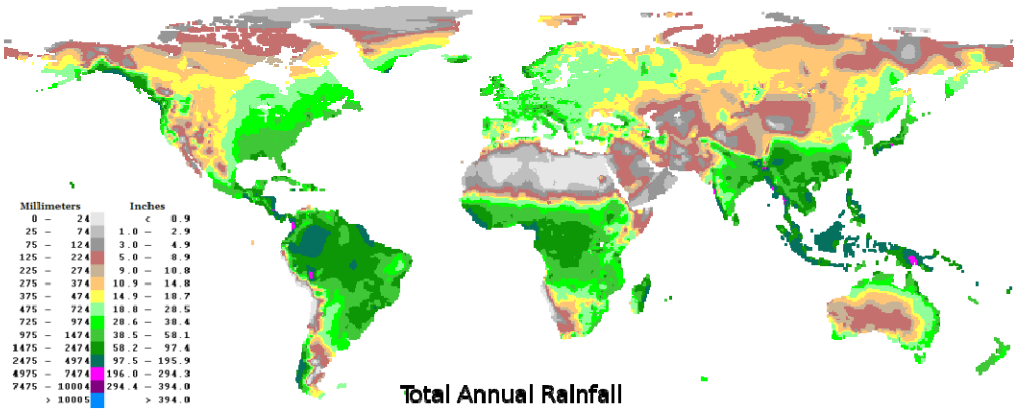

Fig.23. Showing annual rainfall source: NASA.

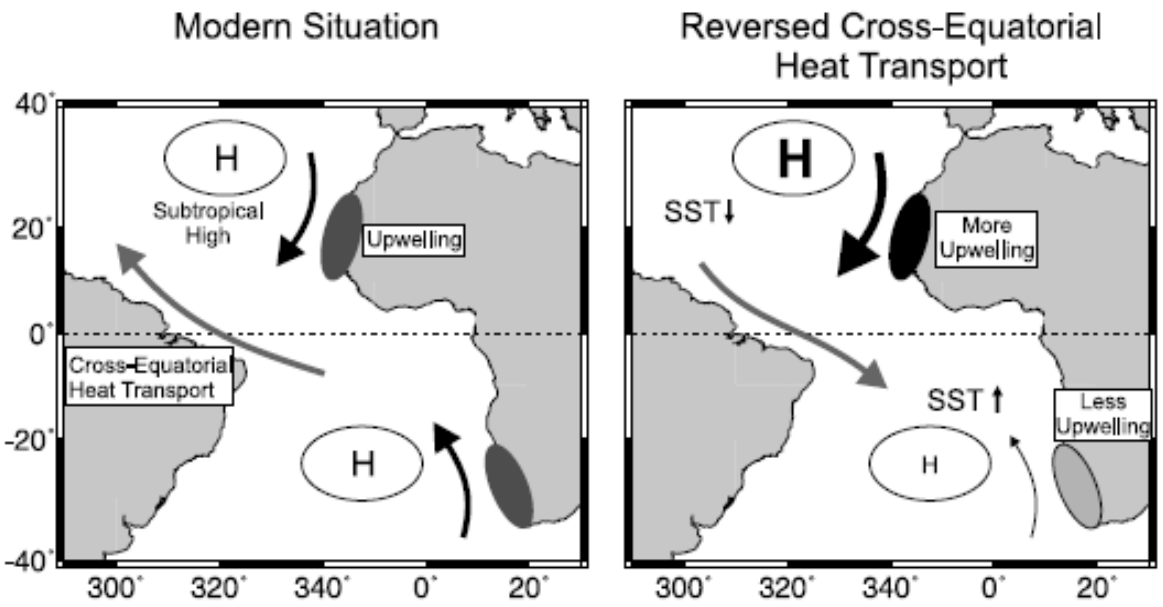

Fig.23a. Showing the upwelling affecting Deserts Source: (Prange and Schulz 2004)

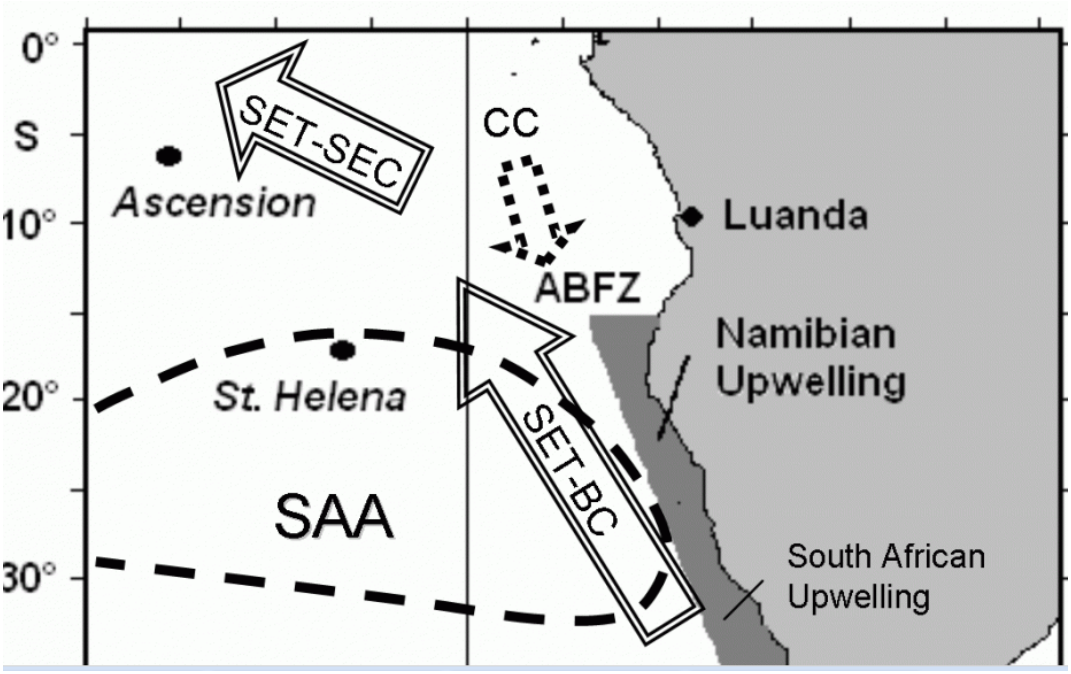

Fig.23b. Namibian upwelling –Kalahari Desert;Source:The Leibniz Institute for Baltic Sea Research, Warnemünde www.io-warnemuende.de/en_hix-st-helena-island

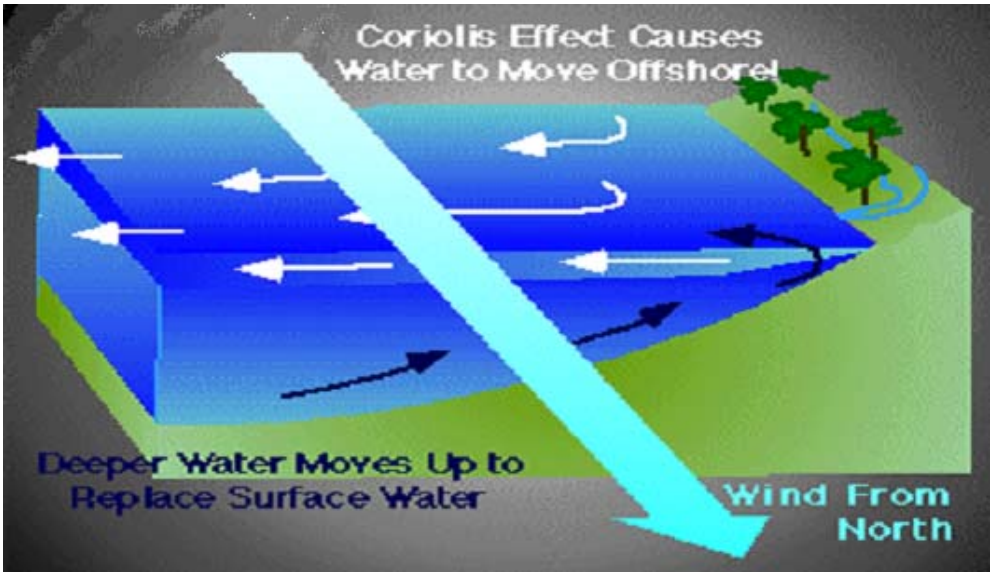

Fig.24. Coastal Upwellings source: *science-house.org*

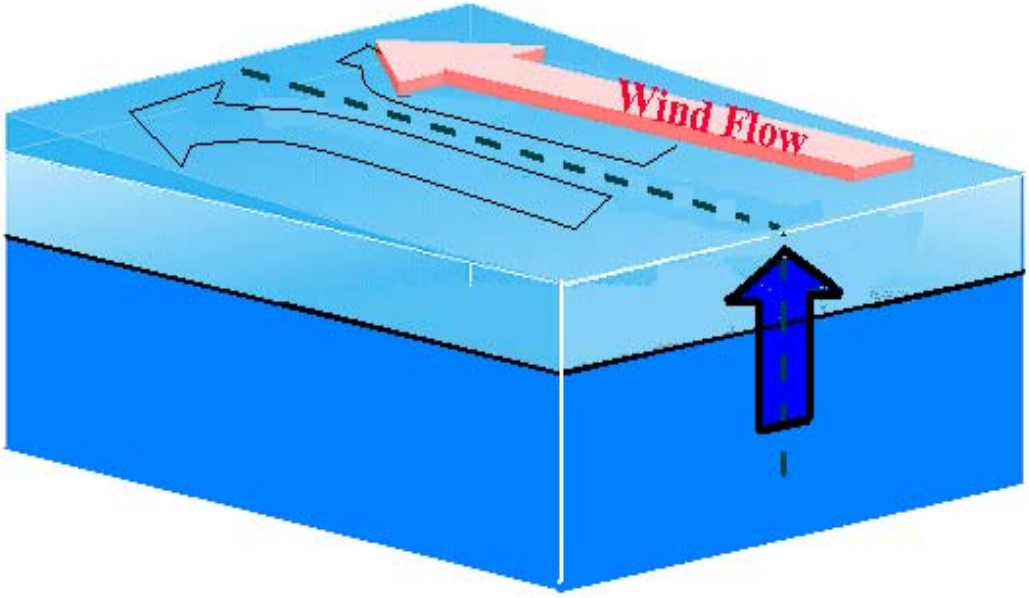

Fig.25. Equatorial Upwelling: source: *science-house.org*

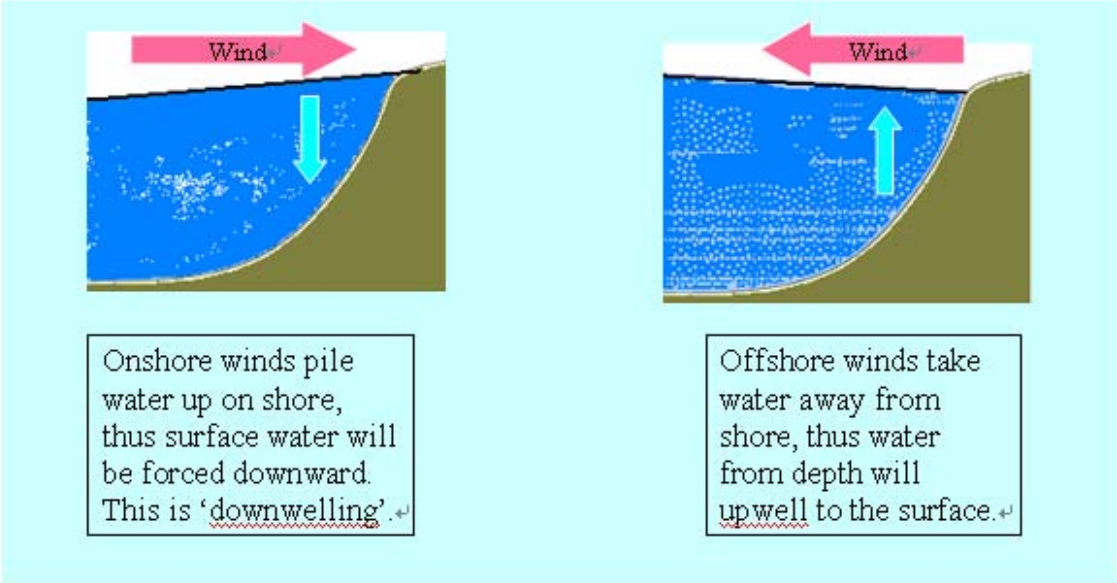

Fig. 26. Seasonal Upwelling. source: *science-house.org*

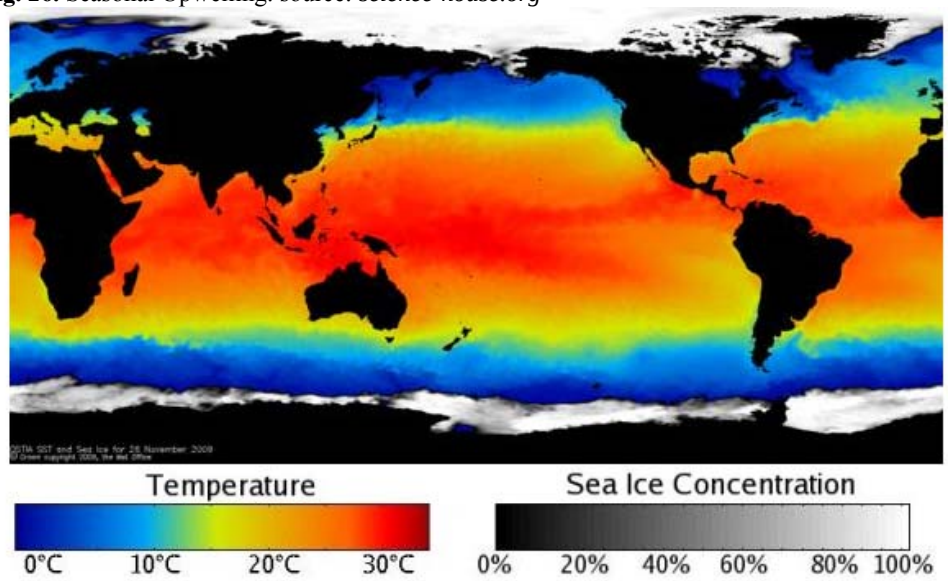

Fig.27. Lattest global sea surface temperature and sea ice analysis updated 17-09-2009 source:NCOF

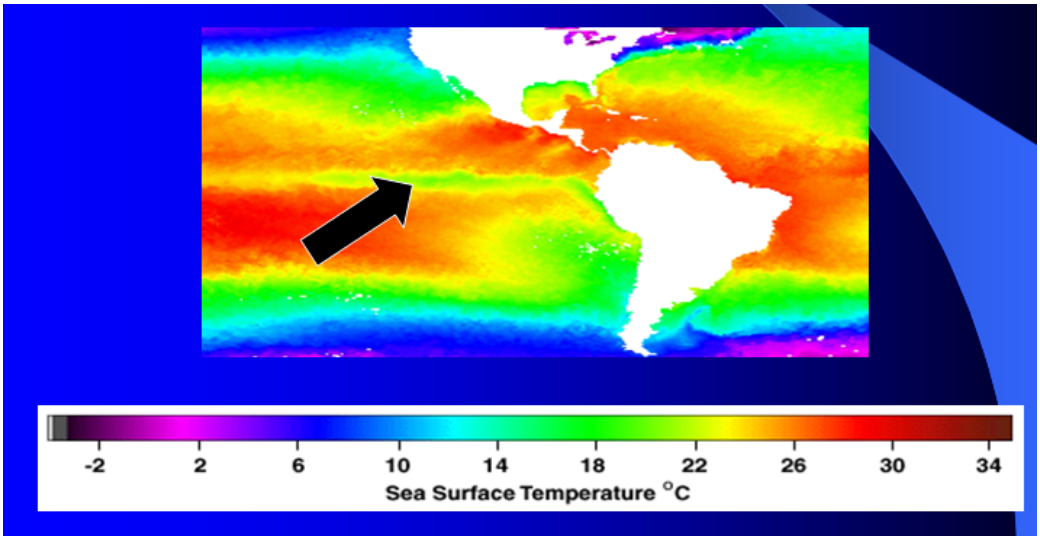

Fig. 28. The deep water that surfaces in upwelling is cold; by looking at Sea Surface Temperature maps we can identify cool upwelled water versus hotter surface water. Source: *science -house.org*

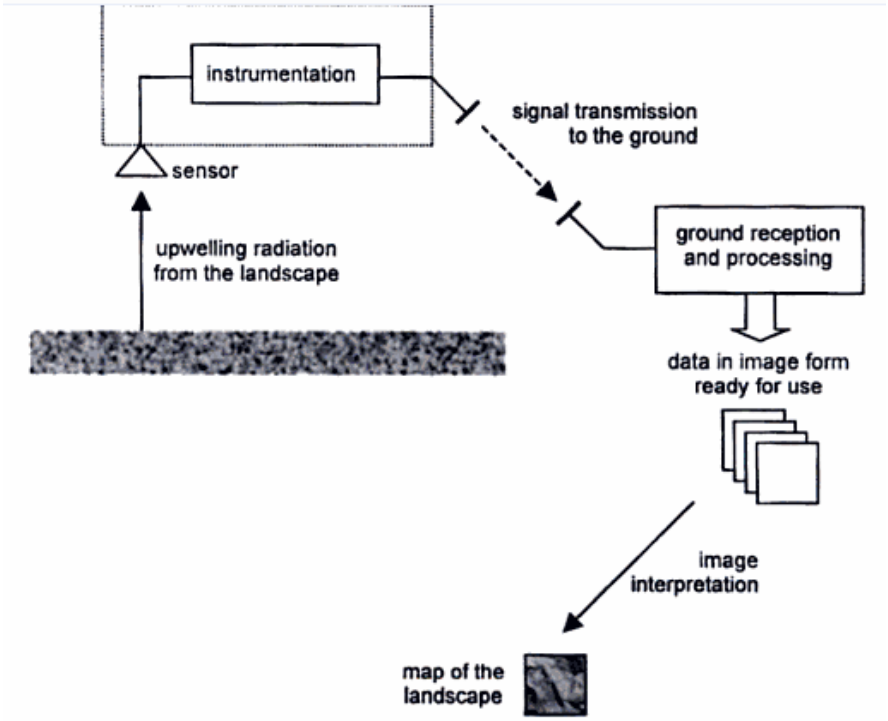

Fig.29 Signal and data flow in a remote control system. Source: (Richards and Jia, 2006).

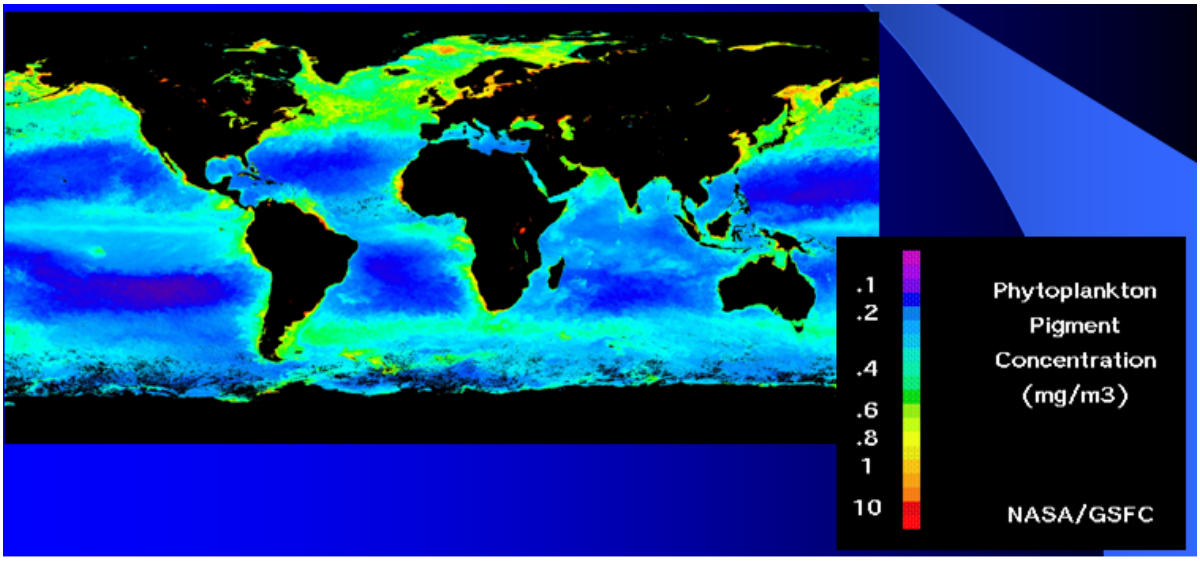

Fig.30. Phytoplankton photosynthesize using specialized color pigments called chlorophyll. Thus, "Ocean Color" maps are another way to identify areas of upwelling. Where on this ocean color map are high phytoplankton concentrations? Source: *science-house.org*

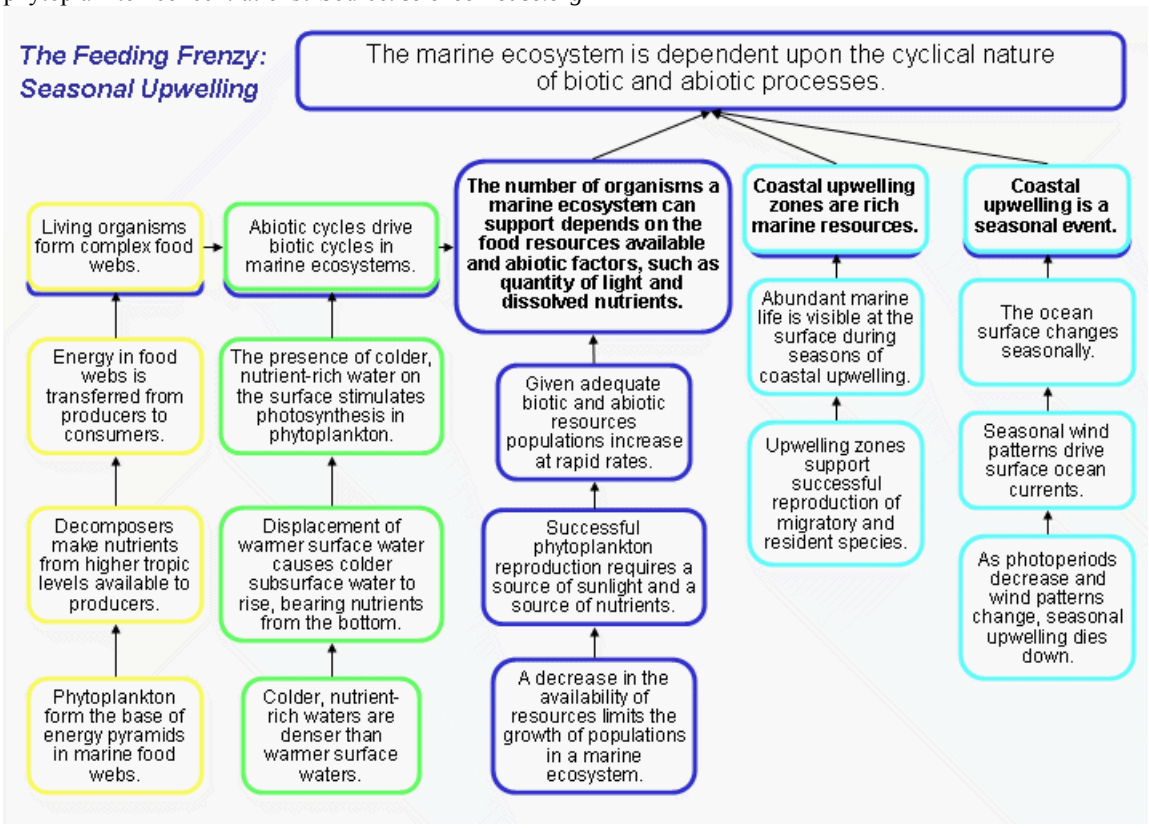

Fig.31. This showing marine ecosystem. Source: DLESE

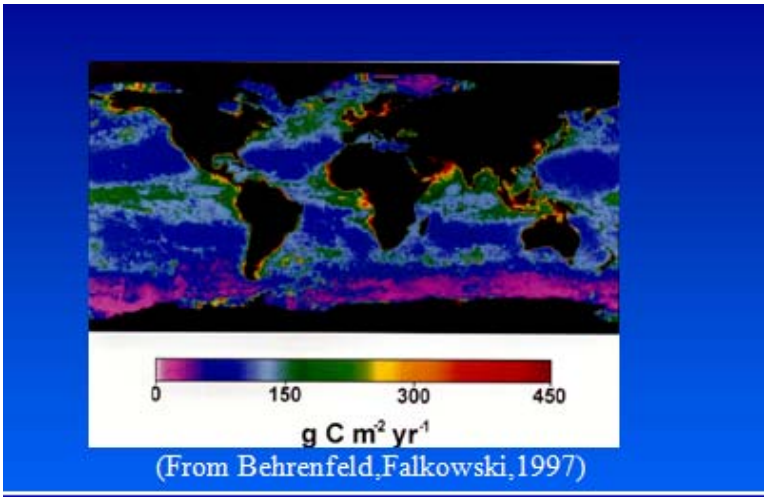

Fig.32. Primary Production image

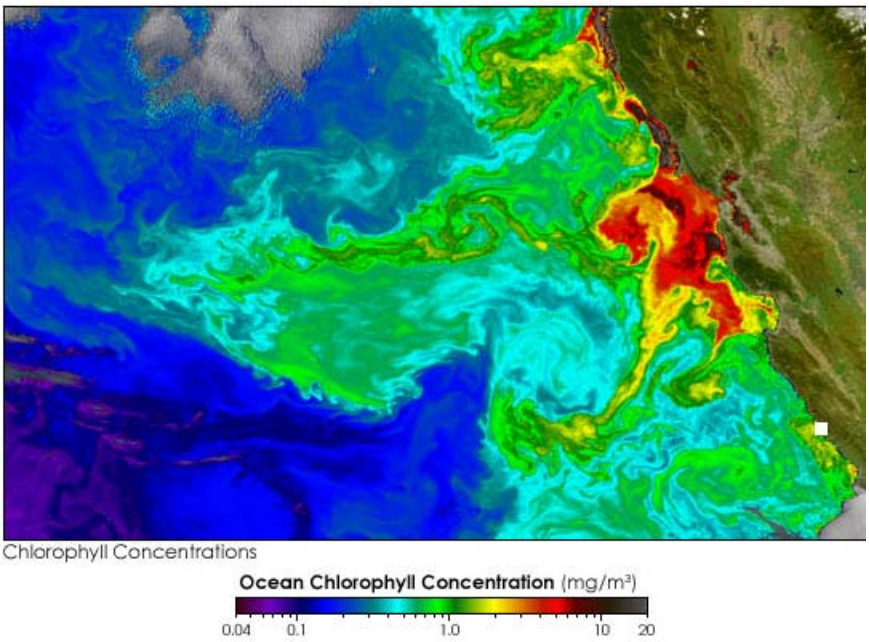

Fig. 33. Ocean chlorophyll concentration off the coast of Sagres .. source: Adapted from NASA

Appendix C. Tables

Table 1. August 2009 Temperature for Computer generated, Sagres weather station and Windguru data.

DATE/TIME	TEMP.LOGGER(ºC)	ICELY WX.(ºC)	WINDGURU TEMP.(ºC)
01-08-2009	16.6 °C		22
02-08-2009	16.4 °C		20
03-08-2009	16.4 °C		22
04-08-2009	15.5 °C		24
05-08-2009	15.8 °C		23
06-08-2009	15.8 °C		22
07-08-2009	15.8 °C		22
08-08-2009	15.9 °C		21
09-08-2009	15.6 °C		22
10-08-2009	16.3 °C		23
11-08-2009	16.2 °C		23
12-08-2009	15.9 °C		24
13-08-2009	16.6 °C		24
14-08-2009	17.7 °C		24
15-08-2009	19.1 °C		24
16-08-2009	20.1 °C		24
17-08-2009	20.3 °C		23
18-08-2009	21.0 °C	26.4	23
19-08-2009	21.2 °C	25.3	23
20-08-2009	20.8 °C	25.1	23
21-08-2009	20.6 °C	21.2	22
22-08-2009	21.1 °C	30.3	25
23-08-2009	21.5 °C	26.6	24
24-08-2009	21.7 °C	22.8	22
25-08-2009	21.6 °C	20.9	21
26-08-2009	19.3 °C	22.9	22
27-08-2009	20.0 °C	25.3	24
28-08-2009	17.4 °C	23.1	23
29-08-2009	17.7 °C	28.3	24
30-08-2009	17.4 °C	27.3	25
31-08-2009	19.3 °C	22.3	23

Table 2. September 2009 Temperature for Computer generated, Sagres weather station and Windguru data .

DATE/TIME	TEMP.LOGGER(ºC)	ICELY WX.(ºC)	WINDGURU/TEMP.(ºC)
01-09-2009	21.2 °C	22.7	21
02-09-2009	19.9 °C	20.2	21
03-09-2009	19.4 °C	23.6	22
04-09-2009	18.2 °C	23.2	23
05-09-2009	17.9 °C	21.3	23
06-09-2009	16.6 °C	27.9	23
07-09-2009	17.2 °C	26.9	24
08-09-2009	19.4 °C	25	24
09-09-2009	20.7 °C	25.2	24
10-09-2009	21.6 °C	25	23
11-09-2009	22.2 °C	26.6	22
12-09-2009	22.4 °C	24.7	22
13-09-2009	22.0 °C	23	21
14-09-2009	22.1 °C	21.3	21
15-09-2009	21.5 °C	21.9	20
16-09-2009	18.9 °C	21.2	22
17-09-2009	16.8 °C	19.3	20
18-09-2009	15.9 °C	20.9	20
19-09-2009	15.4 °C	20.2	20
20-09-2009	15.7 °C	20.4	20
21-09-2009	15.0 °C	21.2	22
22-09-2009	16.4 °C	22.3	23
23-09-2009	17.0 °C	25.3	23
24-09-2009	18.6 °C	23	23
25-09-2009	20.9 °C	23.1	22
26-09-2009	22.5 °C	19.6	21
27-09-2009	21.0 °C	22.3	21
28-09-2009	22.0 °C		22
29-09-2009	22.0 °C		22
30-09-2009	21.0 °C		21

Table 3 October 2009 Temperature for Computer generated, Sagres weather station and Windguru data.

DATE/TIME	TEMP.LOGGER(ºC)	ICELY WX.(ºC)	WINDGURU/TEMP.(ºC)
01.10.2009	22.0		22
02.10.2009	22.0		22
03.10.2009	22.0		22
04.10.2009	22.0		22
05.10.2009	22.0		22
06.10.2009	22.0		22
07.10.2009	22.0		22
08.10.2009	21.0		21

09.10.2009	21.0		21
10.10.2009	22.0	21.3	22
11.10.2009	23.0	25.6	23
12.10.2009	24.0	24.9	24
13.10.2009	23.0	23.3	23
14.10.2009	22.0	22.7	22
15.10.2009	22.0	23.3	22
16.10.2009	22.0	23.1	22
17.10.2009	22.0	22.2	22
18.10.2009	22.0	24.9	22
19.10.2009	20.0	20.0	20
20.10.2009	20.0	18.1	20
21.10.2009	19.0	19.2	19
22.10.2009	21.0	20.4	21
23.10.2009	20.0	20.7	20
24.10.2009	22.0	22.0	22
25.10.2009	22.0	23.6	22
26.10.2009	21.0		21
27.10.2009	22.0		22
28.10.2009	22.0		22
29.10.2009	21.0		21
30.10.2009	21.0		21
31.10.2009	22.0		22

Table4. April mean temperature with missing values and satellite grid data, Sagres Meteorological station.

STATION	STN_SAGRES	GRID1	GRID2	GRID3	GRID4	GRID5
LAT	37	37	39	41	43	37
LONG	-8.93	-15	-15	-15	-15	-13
1990	-999	-0.2	-0.1	-0.1	-0.1	0.8
1991	-999	0.00E+00	0.1	0.1	0.1	1
1992	-999	0.2	0.3	0.2	0.2	1.1
1993	-999	0.4	-0.1	0.4	0.4	1.1
1994	14.5	0.7	0.5	0.6	0.8	0.00E+00
1995	16	0.6	0.6	0.5	0.6	0.1
1996	14.5	0.7	0.7	0.6	0.5	0.4
1997	17.8	1	1.6	0.6	0.6	0.8
1998	15.4	0.00E+00	-0.1	-0.2	-0.2	-0.2
1999	15.2	0.1	-0.1	-0.2	-0.2	-0.2
2000	14.7	0.3	0.00E+00	-0.2	-0.2	0.00E+00
2001	-999	0.2	-0.4	-0.4	-0.3	0.00E+00
2002	-999	-0.7	-0.6	-0.4	-0.2	0.1
2003	-999	-0.7	-0.5	-0.4	-0.3	0.00E+00

2004	-999	-0.6	-0.4	-0.3	-0.3	-0.2
2005	-999	-0.5	0.3	-0.3	-0.4	0.00E+00
2006	-999	1.1	1.1	1.2	1.1	-0.3
2007	-999	1.2	1.2	1.2	1.1	-0.3
2008	-999	1.4	1.5	1.5	1.3	-0.1
2009	14.8	1.6	1.2	1.8	1.7	0.00E+00

Table 5. Replaced missing April data using an example of Sagres Meteorological station.

	STN_SAGRES	GRID1	GRID2	GRID3	GRID4
cpt:Y	37	37	39	41	43
cpt:X	-8.93	-15	-15	-15	-15
1990	16.83882726	-0.2	-0.1	-0.1	-0.1
1991	17.26830428	0	0.1	0.1	0.1
1992	17.48304279	0.2	0.3	0.2	0.2
1993	17.48304279	0.4	-0.1	0.4	0.4
1994	14.5	0.7	0.5	0.6	0.8
1995	16	0.6	0.6	0.5	0.6
1996	14.5	0.7	0.7	0.6	0.5
1997	17.8	1	1.6	0.6	0.6
1998	15.4	0	-0.1	-0.2	-0.2
1999	15.2	0.1	-0.1	-0.2	-0.2
2000	14.7	0.3	0	-0.2	-0.2
2001	15.12091918	0.2	-0.4	-0.4	-0.3
2002	15.33565769	-0.7	-0.6	-0.4	-0.2
2003	15.12091918	-0.7	-0.5	-0.4	-0.3
2004	14.69144216	-0.6	-0.4	-0.3	-0.3
2005	15.12091918	-0.5	0.3	-0.3	-0.4
2006	14.47670365	1.1	1.1	1.2	1.1
2007	14.47670365	1.2	1.2	1.2	1.1
2008	14.90618067	1.4	1.5	1.5	1.3
2009	14.8	1.6	1.2	1.8	1.7

Table 6. Showing the seven variables in 2˚x2˚,for global.

name	title	I	J	K	L
SST	**SEA SURFACE TEMPERATURE**	**1:180**	**1:90**	**1:1**	**1:12**
AIRT	**AIR TEMPERATURE**	**1:180**	**1:90**	**1:1**	**1:12**
SPEH	**SPECIFIC HUMIDITY**	**1:180**	**1:90**	**1:1**	**1:12**
WSPD	**WIND SPEED**	**1:180**	**1:90**	**1:1**	**1:12**
UWND	**ZONAL WIND**	**1:180**	**1:90**	**1:1**	**1:12**
VWND	**MERIDIONAL WIND**	**1:180**	**1:90**	**1:1**	**1:12**
SLP	**SEA LEVEL PRESSURE**	**1:180**	**1:90**	**1:1**	**1:12**

Table 7. Showing windguru speed and direction for three months of August to October 2009

DATE/TIME	SPEED(km/h)	DIRECTION	DIRECTION
01.08.2009	21	112.5	NNW
02.08.2009	29	112.5	NNW
03.08.2009	20	112.5	NNW
04.08.2009	19	112.5	NNW
05.08.2009	26	112.5	NNW
06.08.2009	23	112.5	NNW
07.08.2009	36	112.5	NNW
08.08.2009	36	112.5	NNW
09.08.2009	25	112.5	NNW
10.08.2009	5	112.5	NNW
19.08.2009	14	112.5	NNW
20.08.2009	28	112.5	NNW
21.08.2009	27	112.5	NNW
22.08.2009	11	112.5	NNW
24.08.2009	32	112.5	NNW
25.08.2009	24	112.5	NNW
26.08.2009	16	112.5	NNW
27.08.2009	23	112.5	NNW
28.08.2009	26	112.5	NNW
29.08.2009	14	112.5	NNW
30.08.2009	11	90	N
31.08.2009	13	90	N
03.09.2009	25	112.5	NNW
04.09.2009	34	112.5	NNW
05.09.2009	31	112.5	NNW
06.09.2009	15	112.5	NNW
07.09.2009	13	112.5	NNW
08.09.2009	25	112.5	NNW
09.09.2009	19	67.5	EEN
10.09.2009	27	67.5	EEN
13.09.2009	15	112.5	NNW
14.09.2009	24	112.5	NNW
15.09.2009	19	112.5	NNW
16.09.2009	22	112.5	NNW
17.09.2009	29	112.5	NNW
18.09.2009	16	112.5	NNW
20.09.2009	19	135	NW
21.09.2009	14	135	NW
23.09.2009	3	90	N
24.09.2009	22	292.5	SSE

25.09.2009	13	225	SW
27.09.2009	8	292.5	SSE
28.09.2009	4	360	E
29.09.2009	17	347.5	EES
02.10.2009	4	292.5	SSE
08.10.2009	21	292.5	SSE
09.10.2009	20	270	S
10.10.2009	12	247.5	WWS
11.10.2009	17	112.5	NNW
12.10.2009	16	112.5	NNW
13.10.2009	31	90	N
14.10.2009	20	67.5	NNE
15.10.2009	6	45	NE
16.10.2009	8	45	NE
17.10.2009	16	360	E
18.10.2009	4	360	E
21.10.2009	23	325	SE
24.10.2009	12	225	SW
25.10.2009	19	180	W
26.10.2009	14	247.5	WWS
28.10.2009	22	67.5	NNE
29.10.2009	13	67.5	NNE
30.10.2009	5	360	E
31.10.2009	18	325	SE

Table 8. Showing August 1999 wind direction and Speed for Sagres**.**

DATE	SPEED(km/h)	DIRECTION	SPEED(M/S)
8/1/1999	32	310	8.9
8/2/1999	28	280	7.8
8/3/1999			
8/4/1999			
8/5/1999			
8/6/1999			
8/7/1999			
8/8/1999			
8/9/1999	18	280	5.0
8/10/1999			
8/11/1999			
8/12/1999			
8/13/1999			
8/14/1999			
8/15/1999			

8/16/1999			
8/17/1999			
8/18/1999	18	320	5.0
8/19/1999			
8/20/1999	36	350	10.0
8/21/1999			
8/22/1999			
8/23/1999			
8/24/1999			
8/25/1999			
8/26/1999			
8/27/1999			
8/28/1999	18	320	5.0
8/29/1999	18	310	5.0
8/30/1999	18	300	5.0
8/31/1999	7	240	1.9

Table 9. IRI Probabilistic ENSO Forecast for NINO3.4 Region - Made in September 2009

Season	La Niña	Neutral	El Niño
SON 2009	**1%**	**10%**	**89%**
OND 2009	**1%**	**14%**	**85%**
NDJ 2010	**1%**	**14%**	**85%**
DJF 2010	**1%**	**19%**	**80%**
JFM 2010	**3%**	**24%**	**73%**
FMA 2010	**5%**	**30%**	**65%**
MAM 2010	**10%**	**40%**	**50%**
AMJ 2010	**20%**	**45%**	**35%**
MJJ 2010	**25%**	**50%**	**25%**
JJA 2010	**25%**	**50%**	**25%**

Table 10. August 1999 daily sea temperatures

DATE	TEMP. LOGGER (C°)
8/1/1999	14.5
8/2/1999	14.2
8/3/1999	14.5
8/4/1999	13.8
8/5/1999	13.8
8/6/1999	14.2
8/7/1999	14.5
8/8/1999	15.6
8/9/1999	16
8/10/1999	15.6
8/11/1999	14.5
8/12/1999	14.5
8/13/1999	14.5
8/14/1999	14.9
8/15/1999	14.9
8/16/1999	15.3
8/17/1999	15.6
8/18/1999	14.9
8/19/1999	14.9
8/20/1999	14.5
8/21/1999	14.5
8/22/1999	14.5
8/23/1999	14.2
8/24/1999	14.2
8/25/1999	14.2
8/26/1999	16
8/27/1999	16.7
8/28/1999	16.7
8/29/1999	15.6
8/30/1999	14.9
8/31/1999	14.9